

Third order Møller-Plesset theory made more useful? The role of density functional theory orbitals

Adam Rettig,^{*,†,‡,¶} Diptarka Hait,^{*,†,‡,¶} Luke W. Bertels,^{†,§} and Martin Head-Gordon^{*,†,‡}

[†]*Kenneth S. Pitzer Center for Theoretical Chemistry, Department of Chemistry, University of California, Berkeley, California 94720, USA*

[‡]*Chemical Sciences Division, Lawrence Berkeley National Laboratory, Berkeley, California 94720, USA*

[¶]*These authors contributed equally to this work.*

[§]*Current address: Department of Chemistry, Virginia Tech, Blacksburg, VA 24061, USA*

E-mail: adam_rettig@berkeley.edu; diptarka@berkeley.edu; mhg@cchem.berkeley.edu

Abstract

The practical utility of Møller-Plesset (MP) perturbation theory is severely constrained by the use of Hartree-Fock (HF) orbitals. It has recently been shown that use of regularized orbital-optimized MP2 orbitals and scaling of MP3 energy could lead to a significant reduction in MP3 error (J. Phys. Chem. Lett. 10, 4170, 2019). In this work we examine whether density functional theory (DFT) optimized orbitals can be similarly employed to improve the performance of MP theory at both the MP2 and MP3 levels. We find that use of DFT orbitals leads to significantly improved performance for prediction of thermochemistry, barrier heights, non-covalent interactions,

and dipole moments relative to standard HF based MP theory. Indeed MP3 (with or without scaling) with DFT orbitals is found to surpass the accuracy of coupled cluster singles and doubles (CCSD) for several datasets. We also found that the results are not particularly functional sensitive in most cases, (although range-separated hybrid functionals with low delocalization error perform the best). MP3 based on DFT orbitals thus appears to be an efficient, non-iterative $O(N^6)$ scaling wave function approach for single-reference electronic structure computations. Scaled MP2 with DFT orbitals is also found to be quite accurate in many cases, although modern double hybrid functionals are likely to be considerably more accurate.

1 Introduction

Perturbative approaches offer a straightforward route for inexpensively improving predictions from existing quantum chemistry approximations.¹⁻¹⁰ Perhaps the best known perturbation technique is Møller-Plesset (MP) theory,^{1,2,11} which acts upon a single Slater determinant $|\Phi\rangle$. The zeroth-order Hamiltonian in MP theory is the mean-field one-particle Fock operator \mathbf{F} corresponding to $|\Phi\rangle$ while the remaining terms of the true many-body Hamiltonian \mathbf{H} are treated as a perturbative fluctuation potential \mathbf{U} . The resulting theory is size-consistent at all orders in the fluctuation.¹¹ The energies at all orders are also invariant to rotations between degenerate orbitals, which is not typically true for many other perturbation theories (like Epstein-Nesbet theory^{12,13}). Such alternative theories can consequently predict dramatically different energies for different orbital representations,¹⁴ making MP theory the preferred single reference perturbative approach.

Typically, the reference zeroth-order wave function $|\Phi\rangle$ is a solution to the Hartree-Fock (HF) equations, which leads to the sum of the zeroth and first-order (i.e. MP0 and MP1) energies to be equal to the HF energy E_{HF} . Correlation effects thus arise from higher-order terms by definition, with second-order MP2 perhaps being the simplest wave function based dynamical correlation approach. The historical popularity of MP2 owes a great deal to its

relatively low computational cost, which is asymptotically dominated by the formally $O(N^5)$ scaling cost² of building two electron integrals in the molecular orbital (MO) basis (N being the number of basis functions). MP2 like expressions also arise in density functional theory (DFT) via Görling-Levy perturbation theory.¹⁵ This has led to development of double hybrid density functionals^{16–19} (employing MP2-like expressions within the exchange-correlation contribution) that are amongst the most accurate DFT approximations known to date.^{20,21}

Higher order terms in the MP series are however not as widely used in practice. This is largely a consequence of the slow convergence of the MP series for even apparently single reference problems.² Spin-unrestricted MP theory has long been known to converge extremely slowly, on account of spin-contamination in the UHF orbitals.^{22–24} However, oscillatory behavior around the exact value and even divergent behavior are known to arise for closed-shell systems without spin-symmetry breaking,^{25–27} even for systems as simple as a Ne atom. In practice therefore, predictions from MP theory are not guaranteed to be systematically improvable beyond MP2. However, addition of only a fraction of the third-order energy to MP2 is empirically often found to be effective, leading to an equal interpolation between MP2 and MP3 to gain some popularity as “MP2.5”.²⁸ Nonetheless, MP3 based approaches are less popular than coupled-cluster singles and doubles (CCSD), despite the latter requiring multiple $O(N^6)$ iterations (vs a single $O(N^6)$ scaling step for MP3). This is a consequence of CCSD being also exact to third-order in \mathbf{U} and much better behaved in practice. MP4 is even less competitive due to $O(N^7)$ scaling, although its form inspired the development of the (T) triples correction³ to CCSD, with the resulting CCSD(T) method being widely considered to be the “gold-standard” of single-reference quantum chemistry.

In practice, the use of MP2 has also been hindered by the use of reference HF orbitals.² HF has a propensity for artificially breaking spin-symmetry even for mostly single reference problems, leading to extremely slow convergence of the spin-unrestricted MP series (and subsequent poor performance of MP2).^{22–24} HF also overly localizes electron density due to lack of correlation,^{29,30} which can adversely affect MP2 performance by providing

it with a poor starting point. This has led to the development of orbital optimized MP2 (OOMP2) approaches,^{31–33} where the orbitals are optimized in the presence of MP2 correlation to ameliorate artificial symmetry breaking or overlocalization errors in the reference Slater determinant. In addition, spin-component scaled MP2 methods^{34–36} have also been developed to improve prediction quality, though such approaches cannot be readily extended to spin-general orbitals. Extensions of both orbital optimization and spin-component scaling have also been considered at the MP3 level^{37–40}.

Very recently, some of us have shown that orbitals obtained from a regularized OOMP2 (namely κ -OOMP2⁴¹) could be employed to dramatically improve performance of MP3.⁴² Specifically, use of κ -OOMP2 orbitals and scaling the third-order energy E_{MP3} by 0.8 greatly improved prediction of thermochemistry, barrier heights and non-covalent interactions by over a factor of 3 in most cases (relative to standard MP3/MP2.5), leading to better performance than CCSD over several datasets. The success of this MP2.8: κ -OOMP2 approach raises the question as to whether this improvement is largely the consequence of optimizing orbitals in the presence of MP2 correlation, or if other high quality reference orbitals would yield similar results (with or without scaling). Specifically, it is interesting to consider whether DFT approximations with a low penchant for spin-contamination⁴³ and tunable delocalization error^{44–46} can yield reasonable results. DFT orbitals have been shown to improve performance of CC approaches in many difficult cases^{47–50} and it seems plausible that they would have an even larger impact on MP theory due to lack of iterative singles amplitudes (that mimic orbital relaxation in projected CC theories) in the latter. We consequently examine the performance of both scaled and unscaled MP2 and MP3 with DFT orbitals in this work, focusing on the ability to predict chemically relevant energy differences and dipole moments.

2 Methods

We computed MP energies with DFT orbitals (MP:DFT) via the following protocol:

1. A DFT calculation was run to obtain converged (spin-unrestricted) orbitals, with a stability analysis to guarantee that a minimum in orbital space is reached.
2. \mathbf{F} was built from the converged DFT density matrix, using the HF functional. The HF energy E_{HF} is also found similarly.
3. \mathbf{F} was semi-canonicalized by diagonalizing the occupied-occupied and virtual-virtual blocks separately. Note that the reference Slater determinant/density matrix is unaffected by this process, and the occupied-virtual block of \mathbf{F} remains non-zero in general.
4. MP2 and MP3 energies were computed using the semi-canonicalized orbitals $|\phi_p\rangle$ and the corresponding orbital “energies” $\epsilon_p = \langle \phi_p | \mathbf{F} | \phi_p \rangle$. The effects of the occupied-virtual block of \mathbf{F} was computed at the MP2 level (the so-called non-Brillouin singles contribution) but not the MP3 level, similar to Ref 42. Complete exclusion of singles was considered, but is not presented due to suboptimal behavior, as discussed later (and demonstrated in the Supporting Information).

This approach is superficially similar to xDH double hybrid functionals,^{17,51} where a lower rung functional is employed to generate reference orbitals and a higher rung functional (here MP2/MP3 with/without scaling) is used to compute the final energy from the previously converged orbitals (and their energies) without further optimization. However, we stress that the lower rung orbital energies were not used to compute the MP energies in our protocol, unlike typical xDH functionals. The entire purpose of the DFT calculation here is to provide a good set of occupied orbitals, which are then used to form a HF derived \mathbf{F} operator from which semi-canonical orbitals (and their energies) can be obtained for MP theory. Our energy functional is thus purely wave function based, albeit acting upon a DFT generated reference Slater determinant. This distinction is important due to the relatively small fundamental

gaps predicted by many density functionals (leading to MP overcorrelation in a normal xDH approach⁵²), whose effect should be reduced by use of \mathbf{F} orbital energies obtained from HF.

Based on previous success of spin-component scaled MP2s, MP2.5 and the results of Ref 42, we consider four MP models in the present work:

1. MP2: $E = E_{\text{HF}} + E_{\text{MP2}}$.
2. Scaled MP2 (sMP2): $E = E_{\text{HF}} + c_2 E_{\text{MP2}}$
3. MP3: $E = E_{\text{HF}} + E_{\text{MP2}} + E_{\text{MP3}}$
4. Scaled MP3 (sMP3): $E = E_{\text{HF}} + E_{\text{MP2}} + c_3 E_{\text{MP3}}$

where the scaling parameters $c_{2,3}$ are found from fitting to the training set (here the non multi-reference subset of the W4-11⁵³ thermochemistry dataset).

A fifth model with $E = E_{\text{HF}} + c_2 E_{\text{MP2}} + c_3 E_{\text{MP3}}$ was also considered, but yielded results very similar to model 4 and was thus not considered further (since it involves two empirical parameters, as opposed to one for model 4). Further information about this approach is supplied in the supporting information.

We investigated the performance of MP:DFT in two regimes. The first was an extensive assessment of performance vs CCSD(T) benchmarks for reasonably sized triple zeta basis sets (similar to to Ref 42). The relative computational inexpensiveness of this approach permitted us to assess orbitals obtained from several density functionals like SPW92,^{54,55} PBE,⁵⁶ BLYP,^{57,58} B97M-V,⁵⁹ SCAN,⁶⁰ revM06-L,⁶¹ TPSS,⁶² B3LYP,⁶³ PBE0,⁶⁴ MN15,⁶⁵ CAM-B3LYP,⁶⁶ ω B97X-V⁶⁷ and ω B97M-V.⁶⁸ We also considered the behavior of pure Slater exchange⁵⁴ and HFLYP (100% HF exchange + 100% LYP correlation⁵⁸) over the training set, to understand limiting behavior. The relevant ground state energy calculations were done using the aug-cc-pVTZ basis set,⁶⁹⁻⁷¹ while the aug-cc-pCVTZ^{69,70,72} basis set was employed for dipole moments, in order to be consistent with the CCSD(T)/aug-cc-pCVTZ reference numbers reported in Ref 46. The dipole moments were computed via a centered two point

finite difference formula (the same protocol as Ref 46), using a field strength of magnitude 10^{-4} a.u. The frozen core approximation was not employed for any of these calculations.

The second regime entailed assessment against benchmarks at the complete basis set (CBS) limit, for direct comparison to DFT approaches. Only MP: ω B97M-V and MP:HF were examined, with the CBS limit being estimated via the following protocol:

1. The aug-cc-pV5Z basis E_{HF} was treated as the CBS limit.
2. CBS limit E_{MP2} and E_{MP3} were found from basis set extrapolation using frozen-core aug-cc-pVTZ and aug-cc-pVQZ results. The $E_X = E_\infty + AX^{-3}$ extrapolation formula^{73,74} (where X is basis set cardinality) was employed.
3. The frozen-core correction to E_{MP2} and E_{MP3} were estimated from aug-cc-pCVTZ basis results. Lack of aug-cc-pCVTZ for Br necessitated the use of aug-cc-pwCVQZ basis (obtained from the basis set exchange⁷⁵) for Br (and aug-cc-pCVQZ for other atoms in the relevant systems). The K shell of third period elements was kept frozen throughout (K and L shells for Br).
4. Orbital stability analysis was initially only carried out at the aug-cc-pVTZ level. Stability analysis in larger basis sets was only repeated for species that were found to initially yield unstable solutions at the aug-cc-pVTZ level.

All calculations were done with a development version of the Q-Chem 5.2 package.⁷⁶ The RI approximation^{77,78} was not employed for any MP calculations.

3 Triple Zeta Basis Results

3.1 Training Set

Table 1: Scaling coefficients fit over the nonMR portion of the W4-11 dataset for the scaled MP2 (c_2) and scaled MP3 (c_3) models.

Name	c_2 (sMP2/Model 2)	c_3 (sMP3/Model 4)
κ -OOMP2	0.8465	0.8147
HF	0.9035	0.7157
HFLYP	0.9043	0.6466
Slater	0.8157	0.8703
SPW92	0.8158	0.8753
PBE	0.8207	0.8733
BLYP	0.8174	0.8765
B97M-V	0.8411	0.8189
SCAN	0.8331	0.8619
revM06-L	0.8436	0.8449
TPSS	0.8263	0.8721
B3LYP	0.8332	0.8398
PBE0	0.8409	0.8275
MN15	0.8336	0.8281
CAM-B3LYP	0.8380	0.8260
ω B97X-V	0.8464	0.8023
ω B97M-V	0.8412	0.8012

3.1.1 Scaling Parameters

Scaling parameters for the sMP2 (model 2) and sMP3 (model 4) approaches were obtained via least-squares fitting on CCSD(T) values of the non-multireference (nonMR) subset of the W4-11 dataset.⁵³ The resulting scaling parameters, for orbitals resulting from various functionals, are enumerated in Table 1. Fitted c_2 parameters mostly range between 0.8-0.85, which is consistent with the standard expectation that MP2 overcorrelates and a damping factor is useful.

The inclusion of MP3 energy should ideally ameliorate the MP2 overcorrelation effect, although the MP3 portion of the energy has to be optimally scaled down in practice (similar to MP2.5 and MP2.8: κ -OOMP2) to prevent overcorrection into the undercorrelation regime.

It is thus no longer necessary to scale the second-order term once third-order effects are included. This was empirically observed by us on attempting to simultaneously fit both c_2 and c_3 for model 5, which yielded c_2 very close to 1 (and performance similar to sMP3, like the behavior observed in Ref 42). Table 1 shows that the optimal c_3 coefficients for sMP3 are typically between 0.8-0.9 (with the exception of HF/HFLYP) and roughly decreases with the amount of HF exchange present in the functional. The optimal HF c_3 for the training set was found to be 0.7 (and not 0.5 as in MP2.5), and HFLYP has an even smaller scaling factor at 0.65. It is nonetheless worth noting that most functionals predict c_3 similar to κ -OOMP2 (i.e. close to 0.8), with range separated hybrid functionals being closest in magnitude.

Table 2: Root mean square errors (RMSE), mean signed errors (MSE), and maximum absolute errors (MAX) in kcal/mol for MP:DFT on the training set. CCSD values (HF orbitals, and no extra processing) are also supplied as a reference.

Name	RMSE	MSE	MAX	RMSE	MSE	MAX	RMSE	MSE	MAX	RMSE	MSE	MAX
CCSD	4.9	1.5	20.3									
	MP2			sMP2			MP3			sMP3		
κ -OOMP2	12.4	-3.5	56.8	6.2	-0.2	32.3	3.2	0.3	14.6	1.6	-0.4	5.8
HF	12.0	-5.0	51.1	10.4	-2.7	43.4	9.2	-0.9	38.6	8.5	-2.0	39.5
HFLYP	9.2	-3.9	35.0	7.0	-1.7	29.8	6.6	0.0	25.7	5.0	-1.4	24.2
Slater	15.3	-5.5	72.9	6.8	-0.9	33.3	3.4	-0.6	14.0	2.6	-1.3	8.4
SPW92	15.4	-5.1	72.9	6.7	-0.6	34.2	3.1	-0.4	12.6	2.2	-1.0	7.9
PBE	15.0	-4.9	70.9	6.8	-0.6	35.0	3.0	-0.3	12.6	2.2	-0.9	7.4
BLYP	15.3	-4.9	71.4	6.8	-0.5	35.4	3.0	-0.2	11.9	2.1	-0.8	7.1
B97M-V	12.7	-4.2	59.5	6.0	-0.6	30.1	3.3	0.1	14.4	1.8	-0.7	6.4
SCAN	13.9	-4.9	64.7	6.8	-0.8	33.7	3.3	-0.3	13.4	2.4	-0.9	10.7
revM06-L	12.8	-4.4	59.5	6.3	-0.7	32.1	3.0	-0.0	12.9	1.9	-0.7	5.9
TPSS	14.6	-4.9	69.6	6.9	-0.6	35.5	3.0	-0.3	12.5	2.1	-0.9	7.6
B3LYP	13.5	-4.4	62.9	6.4	-0.5	32.7	3.2	-0.1	13.4	1.9	-0.8	6.6
PBE0	12.9	-4.4	60.5	6.3	-0.7	31.7	3.4	-0.1	14.5	2.1	-0.9	7.6
MN15	13.0	-4.2	60.8	5.9	-0.5	29.9	3.3	0.0	13.8	1.9	-0.7	6.5
CAM-B3LYP	12.9	-4.2	59.8	6.1	-0.5	31.2	3.3	0.0	14.0	1.9	-0.7	6.4
ω B97X-V	12.2	-3.8	56.6	6.0	-0.5	30.5	3.5	0.1	15.1	1.8	-0.6	6.4
ω B97M-V	12.2	-3.8	56.7	5.7	-0.5	28.1	3.5	0.1	15.4	1.8	-0.6	6.4

3.1.2 Training Set Results

Table 2 shows that MP2:HF (i.e. standard MP2 with HF orbitals) has an RMSE of 12 kcal/mol vs CCSD(T). MP2:DFT does not improve this picture—in fact predictions are often significantly degraded when orbitals obtained from local functionals like PBE or TPSS are used. This increased MP2:DFT RMSE (vs MP2:HF) almost completely stems from inclusion of non-Brillouin singles (as shown in the Supporting Information), indicating that the orbital energy differences are not too different from HF values. Scaling alters the picture, with sMP2:HF still having quite high RMSE of 10.4 kcal/mol, but sMP2:DFT reducing it to 6-7 kcal/mol, marking a significant improvement. MSE values show that systematic error is greatly eliminated by scaling (indicating effective overcorrelation in the unscaled case), and the maximum absolute error is also quite reduced. We also observe that orbitals from hybrid functionals like ω B97M-V seem to yield lower error than ones from local functionals, though the overall RMSE variation is small (roughly 1 kcal/mol, comparable to the anticipated accuracy of CCSD(T) itself over a single-reference thermochemistry dataset of this nature), indicating somewhat functional agnostic behavior. However these sMP2:DFT results are not competitive with the best double hybrid^{20,21} or hybrid DFT functionals,^{79,80} for thermochemistry (as shown in Section 5). It is also worth noting that (s)MP2: κ OOMP2 behaves very similarly to (s)MP2:DFT approaches, yielding performance close to that of range separated hybrid functionals.

Table 2 further shows that MP3:HF (standard MP3) has an RMSE of 9.2 kcal/mol and sMP3:HF barely improves upon it, yielding an RMSE of 8.5 kcal/mol. Incredibly, every single density functional (save HFLYP) tested improves upon HF by essentially a factor of 3, in both scaled and unscaled regimes. There is also strikingly low variation between different density functionals (a spread of 0.5-0.6 kcal/mol). In fact, even rung 1 SPW92 LSDA yields about the same accuracy as hybrid functionals, indicating a remarkable level of functional agnosticity. It is also worth noting that MP3:DFT fares fairly decently (RMSE of \sim 3.5 kcal/mol, which is lower than CCSD) and sMP3:DFT only improves performance by about

1 kcal/mol. In fact, scaling appears to add systematic error by increasing the magnitude of the MSE. However, sMP3 does appear to reduce the worst case error, which likely contributes to the lower RMSE. The typical 3 – 3.5 kcal/mol RMSE of MP3:DFT is quite close to the RMSE of 3.2 kcal/mol obtained from MP3: κ -OOMP2, which indicates that most of the improvement from explicitly optimizing orbitals in presence of MP2 correlation is captured by using DFT rather than HF orbitals. The sMP3 models perform similarly as well.

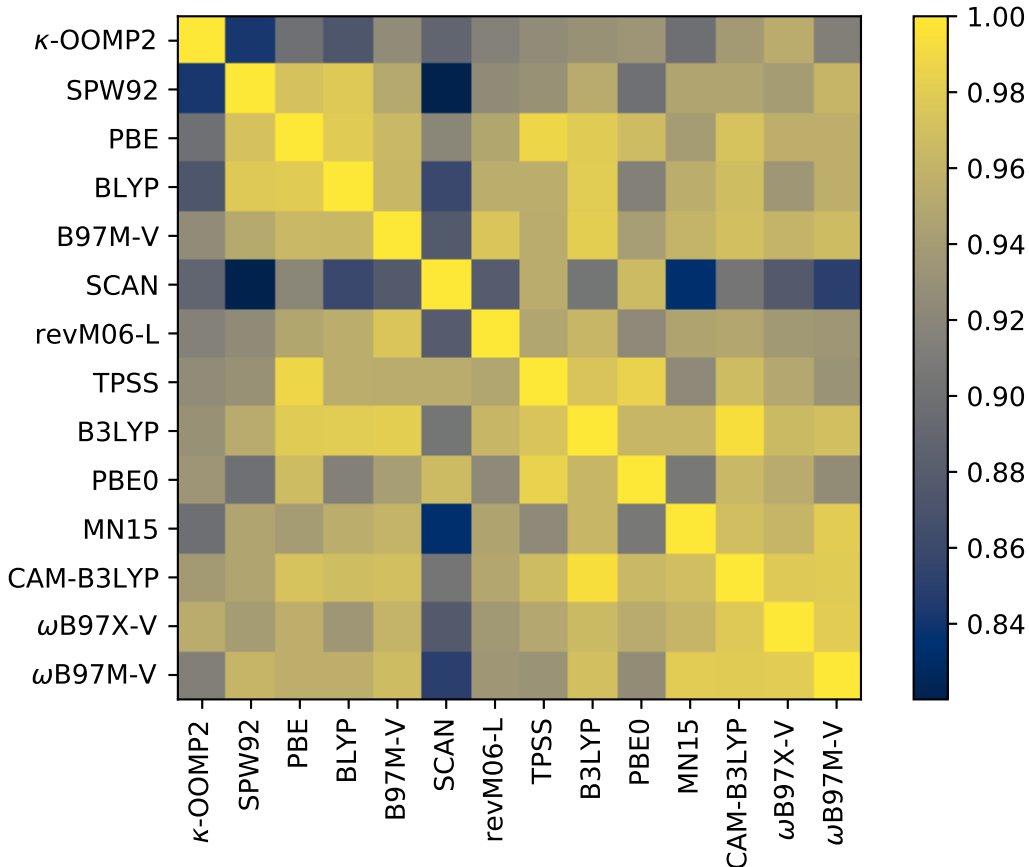


Figure 1: Correlation coefficients computed between sMP3:DFT errors for the non multireference portion of the W4-11 dataset.

This remarkably consistent performance by orbitals generated from many different functionals across the first four rungs of Jacob’s ladder raises the question as to whether the accuracy gains are systematic or whether different functionals are improving performance for different species to different extents, resulting in similar final RMSEs over the whole dataset.

Fig 1 shows the correlation coefficient (r) between sMP3 errors predicted by a characteristic subset of the examined functionals against each other. It is evident that there is quite strong correlation ($r > 0.9$) between errors predicted by most DFT methods. SCAN is somewhat of an outlier, by virtue of having somewhat lower r vs other approaches (and perhaps not so coincidentally, the largest sMP3 RMSE and MAX). Correlation between sMP3:DFT and sMP3: κ -OOMP2 errors is also quite strong ($r > 0.8$ for even local functionals like SPW92). Overall, Fig 1 indicates that the near functional agnosticity of sMP3:DFT is generally a consequence of consistent improvement in predictions over different initial orbital choices (with sMP3: κ -OOMP2 acting similarly as well). The Supporting Information shows that the correlation between sMP3:DFT and CCSD is much lower, showing that the two approaches are improving different aspects over the dataset. Correlation is also low with sMP3:HF or sMP3:HFLYP.

Table 3: Root mean square errors in kcal/mol for MP:DFT on the non-spin contaminated (NSC) and spin contaminated (SC) subsets of the W4-11 dataset. CCSD values (HF orbitals, and no extra processing) are also supplied as a reference.

Name	NSC				SC			
CCSD	4.9				4.9			
	MP2	sMP2	MP3	sMP3	MP2	sMP2	MP3	sMP3
κ -OOMP2	12.2	6.3	3.0	1.5	12.6	6.2	3.4	1.7
HF	8.1	5.4	5.3	2.9	14.9	13.6	11.8	11.7
HFLYP	8.0	5.1	5.1	2.4	10.3	8.5	7.8	6.7
Slater	15.1	6.6	3.0	2.2	15.4	6.9	3.8	2.9
SPW92	15.2	6.7	2.7	2.1	15.5	6.7	3.4	2.3
PBE	14.8	6.7	2.7	1.9	15.2	6.8	3.4	2.4
BLYP	15.1	6.7	2.6	1.9	15.5	6.7	3.3	2.2
B97M-V	12.5	6.0	3.1	1.7	12.9	6.1	3.5	1.9
SCAN	13.5	6.4	2.8	1.7	14.3	7.0	3.7	3.0
revM06-L	12.8	6.3	2.8	1.8	12.9	6.2	3.3	2.1
TPSS	14.3	6.8	2.6	1.8	14.8	6.9	3.4	2.4
B3LYP	13.3	6.3	2.9	1.7	13.7	6.3	3.5	2.1
PBE0	12.7	6.2	3.0	1.7	13.1	6.4	3.6	2.4
MN15	13.0	6.0	3.0	1.8	12.9	5.8	3.5	1.9
CAM-B3LYP	12.8	6.1	3.0	1.7	13.1	6.1	3.5	2.0
ω B97X-V	12.1	6.0	3.2	1.7	12.2	5.9	3.7	1.9
ω B97M-V	12.2	5.7	3.3	1.8	12.3	5.6	3.7	1.9

3.1.3 Role of spin-contamination

A natural question to consider is whether the significant accuracy gains stem mostly from DFT functionals lowering spin-contamination, or whether other factors are also at play. This can be addressed by dividing the nonMR W4-11 energies into non spin-contaminated (NSC) and spin-contaminated (SC) subsets. An energy is classified as NSC if all of the participating species have HF $\langle S^2 \rangle$ values that deviate by no more than 10% from the exact, spin-pure $\langle S^2 \rangle$ value. The remaining energies are classified as SC, with the NSC and SC subsets having 373 and 372 reaction energies respectively. Table 3 presents the RMSEs predicted with various approaches for these subsets. The performance of CCSD is nearly the same across both subsets, likely as a consequence of the removal of the explicitly multireference species from W4-11. However, there is a significant degradation in performance of MP:HF on moving from the NSC to SC subset, leading to an increase in RMSE by $\sim 7-9$ kcal/mol.

Use of DFT orbitals however greatly ameliorates this issue, with MP:DFT methods (save MP:HFLYP) yielding fairly similar RMSEs over both subsets (although errors are slightly larger for the SC subset). This leads to significantly better sMP2, MP3 and sMP3 results over the SC subset relative to HF, highlighting the importance of reducing spin-contamination. However, it is also worth noting that MP3:DFT has ~ 3 kcal/mol RMSE over the NSC subset vs 5 kcal/mol RMSE for MP3:HF, showing that errors are reduced even in the absence of spin-contamination. Similarly, sMP3:DFT with meta-GGA and hybrid functionals reduces the sMP3:HF RMSE by 1 kcal/mol over the NSC subset. κ -OOMP2 orbitals yield similar behavior across both subsets, reproducing CCSD(T) to a slightly better extent than DFT methods. It thus appears that while reduction of spin-contamination is an important reason for improved performance of MP:DFT (or MP: κ -OOMP2) over MP:HF, it is not the sole reason as prediction quality is also improved for non spin-contaminated species as well, albeit to a smaller extent.

Table 4: Root mean square errors (RMSE), mean signed errors (MSE), and maximum absolute errors (MAX) in kcal/mol for MP:DFT on the BH76RC dataset.

Name	RMSE	MSE	MAX	RMSE	MSE	MAX	RMSE	MSE	MAX	RMSE	MSE	MAX
CCSD	1.9	-0.6	7.2									
	MP2			sMP2			MP3			sMP3		
κ -OOMP2	6.2	1.0	24.0	3.8	0.8	14.6	1.6	-0.4	6.2	0.8	-0.2	1.5
HF	6.3	-0.1	21.2	5.6	-0.1	21.6	4.5	-1.0	21.6	4.3	-0.7	21.5
SPW92	7.3	1.4	28.7	4.0	1.0	15.8	1.6	-0.4	6.0	1.0	-0.2	2.1
PBE	7.2	1.4	28.6	4.0	1.0	16.1	1.6	-0.4	5.8	0.9	-0.2	2.0
BLYP	7.4	1.4	28.9	4.1	1.0	16.1	1.6	-0.4	5.8	0.9	-0.2	2.1
B97M-V	6.3	1.2	25.2	3.7	0.9	14.9	1.7	-0.4	6.3	0.8	-0.1	1.8
SCAN	6.8	1.4	27.1	4.0	1.0	15.9	1.6	-0.3	5.7	0.9	-0.1	2.2
revM06-L	6.5	1.3	25.7	3.9	1.0	15.6	1.6	-0.3	5.7	1.0	-0.0	2.2
TPSS	7.1	1.4	28.4	4.1	1.0	16.3	1.5	-0.4	5.6	0.9	-0.2	2.1
B3LYP	6.5	1.1	25.2	3.8	0.8	14.6	1.6	-0.5	6.0	0.9	-0.2	1.8
PBE0	6.2	1.1	24.0	3.7	0.8	14.3	1.7	-0.4	6.1	0.9	-0.2	2.0
MN15	6.1	0.9	23.0	3.5	0.7	13.1	1.8	-0.6	6.6	0.9	-0.3	1.9
CAM-B3LYP	6.2	1.0	23.0	3.7	0.7	13.4	1.7	-0.5	6.4	0.9	-0.3	1.7
ω B97X-V	5.9	0.9	21.6	3.6	0.7	12.9	1.8	-0.5	6.7	0.9	-0.2	1.6
ω B97M-V	5.7	0.8	21.1	3.4	0.6	12.2	1.8	-0.6	7.0	0.9	-0.3	1.6

3.2 Test Sets

3.2.1 Thermochemistry

The behavior of MP:DFT (as well as the transferability of the fit coefficients) for other thermochemistry was tested using the BH76RC⁸¹⁻⁸³ and RSE43^{84,85} datasets. The BH76RC dataset consists of the overall reaction energies obtained by taking the difference of the forward and reverse barrier heights in the HTBH38 and NHTBH38 datasets. Table 4 shows that the RMSEs for this dataset present a very similar picture as W4-11. MP2:DFT tends to fare worse than MP2:HF, but scaling leads to a significant improvement in performance (lowering RMSE by ~ 2 kcal/mol). MP3:DFT however marks a significant improvement over MP3:HF (by almost a factor of 3), with the resulting RMSE of ~ 1.7 kcal/mol being competitive with CCSD. sMP3:DFT fares even better, giving RMSEs of less than 1 kcal/mol, compared to 4.3 kcal/mol with sMP3:HF (or 1.9 kcal/mol from CCSD). There is also fairly low variation in predictions from orbitals generated from different functionals for the sMP2, and (s)MP3

approaches.

Table 5: Root mean square errors (RMSE), mean signed errors (MSE), and maximum absolute errors (MAX) in kcal/mol for MP:DFT on the RSE43 dataset.

Name	RMSE	MSE	MAX	RMSE	MSE	MAX	RMSE	MSE	MAX	RMSE	MSE	MAX
CCSD	0.4	0.3	1.0									
	MP2			sMP2			MP3			sMP3		
κ -OOMP2	1.3	-1.0	3.0	0.5	-0.4	1.4	0.5	-0.4	1.6	0.6	-0.5	1.7
HF	4.1	2.3	16.4	3.7	2.2	14.5	2.4	1.6	9.3	2.9	1.8	11.4
SPW92	2.6	-2.3	5.8	0.9	-0.7	2.5	1.0	-0.9	2.2	1.1	-1.0	2.6
PBE	2.3	-2.1	5.2	0.9	-0.7	2.4	1.0	-0.9	2.4	1.2	-1.1	2.7
BLYP	2.4	-2.1	5.3	0.9	-0.7	2.4	1.0	-0.9	2.3	1.2	-1.0	2.7
B97M-V	1.9	-1.6	4.0	0.8	-0.7	2.0	0.9	-0.8	2.3	1.1	-1.0	2.6
SCAN	1.6	-1.2	3.5	0.7	-0.4	2.0	0.8	-0.7	2.1	0.9	-0.8	2.1
revM06-L	1.9	-1.6	4.1	0.9	-0.7	2.0	1.1	-1.0	2.6	1.2	-1.1	2.8
TPSS	2.0	-1.8	4.6	0.8	-0.6	2.2	1.0	-0.9	2.4	1.1	-1.0	2.7
B3LYP	1.8	-1.5	3.6	0.7	-0.6	1.7	0.9	-0.7	2.2	1.0	-0.9	2.4
PBE0	1.5	-1.3	3.1	0.6	-0.5	1.3	0.8	-0.7	2.1	0.9	-0.8	2.2
MN15	1.6	-1.3	3.3	0.6	-0.5	1.3	0.8	-0.7	2.0	0.9	-0.8	2.1
CAM-B3LYP	1.4	-1.2	2.9	0.6	-0.4	1.3	0.7	-0.6	1.8	0.8	-0.7	1.9
ω B97X-V	1.3	-1.1	2.8	0.6	-0.4	1.3	0.6	-0.5	1.6	0.7	-0.6	1.7
ω B97M-V	1.4	-1.2	2.8	0.6	-0.4	1.3	0.7	-0.5	1.7	0.8	-0.7	1.9

The RSE43 dataset consists of reaction energies for hydrogen abstraction of hydrocarbons (by a methyl radical). Table 5 shows somewhat different behavior than the datasets considered previously. MP2:DFT improves significantly over MP2:HF, with several methods reducing RMSE by nearly a factor of 3. This is likely on account of the DFT approaches significantly reducing spin-contamination effects in the reference, which degrades the performance of standard MP2.²⁴ The role of spin-contamination in degrading MP2:HF predictions can be gauged by exclusion of reactions involving heavily spin-contaminated species from the dataset. Nine radicals are found to have UHF $\langle S^2 \rangle \geq 0.9$ vs the ideal value of 0.75 (with the benzyl radical being an extreme case with UHF $\langle S^2 \rangle \sim 1.3$) and three singlet organic molecules are found to have UHF $\langle S^2 \rangle \geq 0$; discarding reactions involving these species (9 reactions in total) lowers MP2:HF RMSE to 1 kcal/mol. The effect on MP2:DFT RMSEs is much more muted (as can be seen from the supporting information), due to significantly lower spin-contamination with the tested DFT functionals (with benzyl radical again being

the worst case, with a SCAN $\langle S^2 \rangle$ of 0.86). Scaling further reduces RMSE (over the full dataset) by a roughly a factor of 2, with sMP2:DFT approaches having RMSE below 1 kcal/mol and being fairly competitive with CCSD (the best functionals yielding an RMSE of 0.6 kcal/mol and CCSD 0.4 kcal/mol).

Moving on to third-order, the performance of MP3:HF is also negatively affected by the spin-contamination in HF orbitals, resulting in a fairly large RMSE of 2.4 kcal/mol (vs 0.9 kcal/mol when the nine most spin-contaminated species are removed). MP3:DFT brings down the RMSE by a factor of 2-3, although sMP3:DFT offers no further improvement in performance. Indeed, (s)MP3 models do not improve upon sMP2 for this dataset, indicating that the excellent performance of sMP2:DFT may be somewhat fortuitous. The (s)MP3:DFT RMSEs show somewhat stronger functional dependence for this dataset (relative to preceding ones), with hybrid functionals reproducing CCSD(T) values somewhat better than local functionals. The overall effect is small in absolute terms (~ 0.5 kcal/mol spread of RMSE, comparable to the W4-11 spread) but is significant in percentage terms—with ω B97X-V having essentially half the RMSE of revM06-L. This argues for use of hybrid functionals for orbital generation (over local functionals). It is also worth noting that use of κ -OOMP2 orbitals reproduces the CCSD(T) benchmark for RSE43 to a slightly (but perceptibly) better extent than the tested functionals.

3.2.2 Kinetics

The performance of the MP:DFT models in predicting reaction kinetics was tested via the HTBH38⁸² and NHTBH38⁸³ datasets, consisting of 38 hydrogen-transfer and non-hydrogen transfer barrier heights respectively. In the case of HTBH38, MP2:DFT does not represent an improvement over standard MP2, but sMP2:DFT fares quite well, halving the RMSE and yielding performance comparable to CCSD. Inclusion of third-order contributions further improves performance, with MP3:DFT having RMSEs ranging from 0.8 – 1.6 kcal/mol vs the CCSD(T) benchmark. These results exhibit greater functional sensitivity than W4-11 or

Table 6: Root mean square errors (RMSE), mean signed errors (MSE), and max absolute errors (MAX) in kcal/mol for MP2.n:DFT on the HTBH38 dataset.

Name	RMSE	MSE	MAX	RMSE	MSE	MAX	RMSE	MSE	MAX	RMSE	MSE	MAX
CCSD	2.2	1.9	4.1									
	MP2			sMP2			MP3			sMP3		
κ -OOMP2	4.0	-2.0	8.7	2.2	0.8	5.5	0.7	0.3	1.8	0.7	-0.1	1.4
HF	4.0	3.0	12.1	4.6	4.0	10.3	3.9	3.5	7.2	3.7	3.4	6.3
SPW92	7.6	-5.0	24.2	2.9	0.2	8.6	1.4	-0.6	5.1	1.9	-1.1	7.4
PBE	6.8	-4.5	20.3	2.6	0.2	7.2	1.5	-0.7	5.2	1.9	-1.2	7.1
BLYP	7.2	-4.7	22.1	2.8	0.2	7.9	1.6	-0.8	5.8	2.1	-1.3	7.8
B97M-V	4.8	-3.2	9.7	2.1	0.4	4.0	1.1	-0.5	3.1	1.4	-1.0	4.2
SCAN	5.0	-3.2	10.7	2.2	0.4	4.5	1.1	-0.4	3.4	1.3	-0.8	4.3
revM06-L	4.7	-3.0	9.6	2.2	0.4	4.4	1.1	-0.5	3.0	1.3	-0.9	3.7
TPSS	5.8	-3.7	15.1	2.4	0.4	4.9	1.3	-0.5	4.4	1.6	-0.9	5.8
B3LYP	4.9	-3.2	10.1	2.1	0.4	4.7	1.0	-0.4	2.8	1.3	-0.8	3.9
PBE0	4.4	-2.7	9.0	2.1	0.5	4.7	0.9	-0.2	2.2	1.0	-0.6	2.9
MN15	4.6	-3.0	9.8	2.0	0.5	4.6	1.0	-0.4	2.6	1.1	-0.9	2.6
CAM-B3LYP	4.4	-2.6	9.0	2.1	0.6	4.8	0.8	-0.1	2.1	0.9	-0.6	2.4
ω B97X-V	4.0	-2.3	8.2	2.1	0.7	4.8	0.8	0.1	2.1	0.7	-0.4	1.9
ω B97M-V	4.2	-2.6	8.6	2.0	0.5	4.5	0.8	-0.2	2.5	0.9	-0.7	2.1

BH76RC (but similar to RSE43), with spread in RMSEs being 0.8 kcal/mol and the ratio of the largest RMSE to smallest being 2. The overall performance of MP3 is generally degraded by the scaling (significantly for local functionals, less so for hybrids), with the range of RMSEs being 0.7 – 2.1 kcal/mol. LSDA/GGAs perform the poorest, while hybrids have the smallest RMS deviation from the CCSD(T) benchmark. Meta-GGAs like SCAN/B97M-V reduce the error significantly relative to LSDA/GGAs, for both the unscaled and scaled models (with TPSS yielding performance between LSDA/GGA and more modern meta-GGAs). However, meta-GGAs still have larger sMP3 RMSE than hybrids in general.

This significant difference in performance based on functional rung is nicely illustrated by the correlation coefficients computed between each functional for the HTBH38 dataset (plotted in Fig. 2). There is clearly reduced correlation between LSDA/GGA and hybrids, with meta-GGAs occupying an intermediate spot. Indeed, correlation with κ -OOMP2 effectively provides a visual representation of Jacob’s ladder. The ability of hybrid functionals to reproduce CCSD(T) values more accurately relative to local functionals may stem from

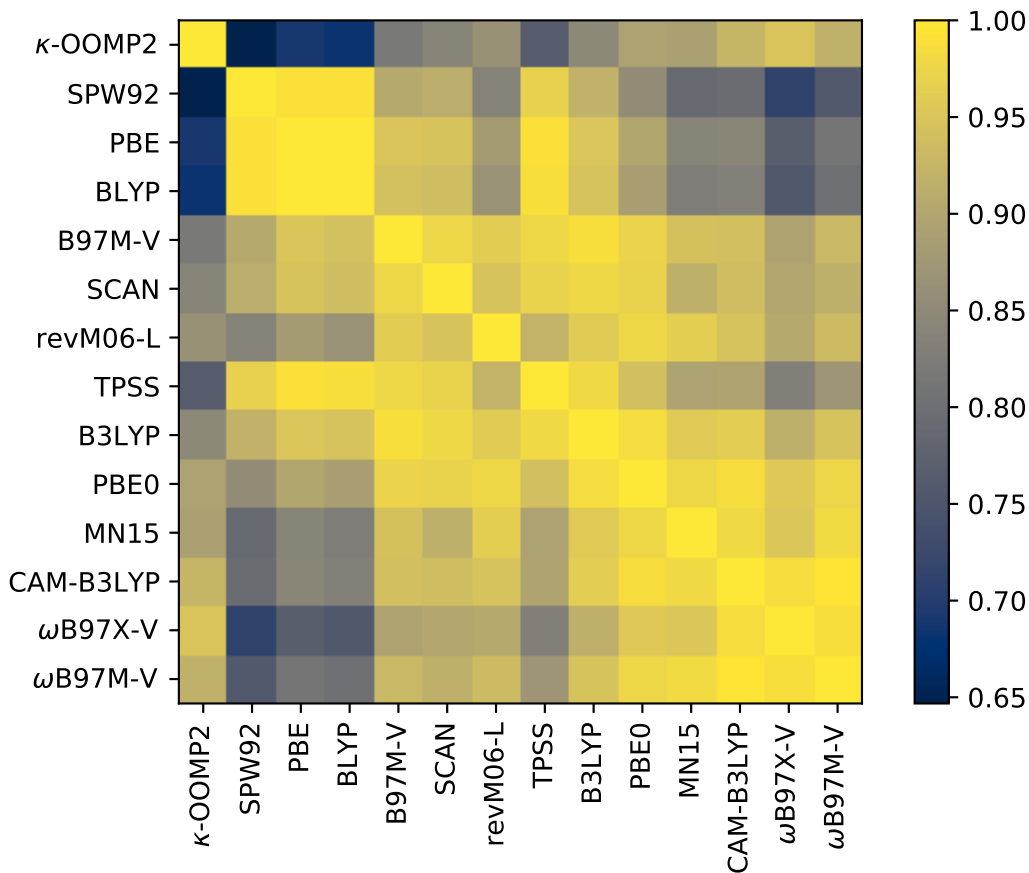


Figure 2: Correlation coefficients computed between SMP3:DFT errors for the HTBH38 dataset.

the underlying delocalization error in the reference functional. Transition states have more ‘fractional charge’ character than equilibrium geometries,⁴⁵ making DFT modeling of barrier heights somewhat more challenging than ground state thermochemistry. Indeed, a number of functionals with increased HF exchange contributions were explicitly developed for improving barrier height predictions.^{86–88} It thus appears that reference orbitals with reduced delocalization error are superior for improving performance of MP theory. However *all* choices of DFT orbitals perform much better than the overly localized HF orbitals.

The NHTBH38 dataset presents a similar picture (except that SMP2:DFT is perceptibly worse than CCSD in this case). The SMP3 results exhibit a similar level of functional dependence as well, further highlighting the delocalization driven challenges associated with

Table 7: Root mean square errors (RMSE), mean signed errors (MSE), and maximum absolute errors (MAX) in kcal/mol for MP:DFT on the NHTBH38 dataset.

Name	RMSE	MSE	MAX	RMSE	MSE	MAX	RMSE	MSE	MAX	RMSE	MSE	MAX
CCSD	2.5	2.1	7.6									
	MP2			sMP2			MP3			sMP3		
κ -OOMP2	5.2	-3.0	21.8	2.9	-0.6	10.5	1.7	1.1	7.2	0.8	0.3	1.8
HF	7.0	4.4	25.6	7.1	4.8	25.0	6.7	5.2	23.3	6.6	4.9	24.0
SPW92	8.0	-5.5	23.7	4.1	-1.1	8.6	1.8	-0.1	5.2	1.9	-0.8	4.1
PBE	7.7	-5.2	24.1	3.9	-1.2	9.5	1.6	-0.2	4.8	1.7	-0.8	3.8
BLYP	7.7	-5.2	24.4	3.8	-1.1	9.4	1.5	-0.2	4.5	1.6	-0.8	3.5
B97M-V	6.1	-3.9	21.1	3.2	-0.8	8.9	1.3	0.2	5.1	1.1	-0.5	2.7
SCAN	6.7	-4.1	22.3	3.6	-0.9	9.4	1.4	0.2	4.9	1.4	-0.4	3.0
revM06-L	6.2	-3.9	21.6	3.3	-0.8	9.6	1.3	0.3	4.8	1.1	-0.4	2.4
TPSS	7.1	-4.6	23.9	3.7	-1.0	10.0	1.4	-0.0	4.7	1.4	-0.6	3.3
B3LYP	6.1	-3.9	20.7	3.3	-0.8	8.4	1.3	0.3	4.9	1.1	-0.4	2.4
PBE0	5.7	-3.6	19.5	3.2	-0.8	8.2	1.4	0.4	5.3	1.1	-0.3	2.4
MN15	5.3	-3.4	19.0	2.7	-0.6	7.3	1.4	0.6	5.4	0.7	-0.1	1.7
CAM-B3LYP	5.2	-3.2	18.5	2.9	-0.5	7.3	1.4	0.6	5.3	0.8	-0.0	1.7
ω B97X-V	4.8	-2.8	17.5	2.7	-0.4	7.3	1.5	0.8	5.8	0.7	0.1	1.3
ω B97M-V	4.9	-3.1	17.7	2.7	-0.5	7.0	1.4	0.7	5.8	0.7	-0.1	1.4

barrier heights (however unscaled MP3:DFT values show significantly less variation). Interestingly, sMP3 performs better than MP3 for hybrid functionals, while little to no benefit is obtained from scaling for local functionals.

3.2.3 Non-covalent Interactions

The applicability of MP:DFT for predicting non-covalent interactions was tested via the TA13⁸⁹ and A24⁹⁰ datasets. The results were counterpoise corrected to account for the small basis set size (as was the CCSD(T) benchmark). TA13 consists of nonbonded interaction energies for small radicals with closed-shell species. MP2:DFT again performs worse than MP2:HF, but scaling greatly improves performance, resulting in RMSE \sim 1 kcal/mol for sMP2:DFT. No systematic behavior with rungs of Jacob’s ladder is seen, with the SPW92 LSDA functional being one of the best performers. Interestingly, third-order contributions do not perceptibly improve predictions as both MP3 and sMP3 approaches have quite similar RMSE as sMP2. sMP3:DFT in fact slightly worsens predictions relative to MP3:DFT, with

Table 8: Root mean square errors (RMSE), mean signed errors (MSE), and maximum absolute errors (MAX) in kcal/mol for MP:DFT on the TA13 dataset.

Name	RMSE	MSE	MAX	RMSE	MSE	MAX	RMSE	MSE	MAX	RMSE	MSE	MAX
CCSD	0.72	0.54	1.47									
	MP2			sMP2			MP3			sMP3		
κ -OOMP2	1.57	-0.53	4.95	0.78	0.14	1.74	0.81	-0.44	2.46	0.82	-0.46	2.08
HF	1.79	0.16	5.16	1.64	0.45	3.93	1.44	0.39	4.00	1.49	0.33	3.84
SPW92	3.29	-2.10	9.21	0.82	0.38	1.69	0.80	-0.49	2.41	0.88	-0.69	2.18
PBE	3.17	-1.80	9.37	0.79	0.20	1.56	0.77	-0.56	2.17	0.93	-0.72	1.95
BLYP	3.23	-1.74	9.58	0.89	0.27	1.92	0.78	-0.56	2.18	0.93	-0.71	1.95
B97M-V	2.80	-1.47	8.31	1.06	-0.09	2.77	0.87	-0.61	2.15	1.15	-0.77	3.27
SCAN	2.92	-1.68	8.68	0.87	-0.14	2.49	0.87	-0.66	1.96	1.10	-0.80	2.88
revM06-L	2.78	-1.50	8.33	0.98	-0.20	2.88	0.90	-0.61	2.26	1.15	-0.75	3.20
TPSS	3.05	-1.70	9.10	0.80	0.07	1.93	0.81	-0.60	1.99	0.99	-0.74	2.28
B3LYP	2.77	-1.46	8.27	0.97	-0.08	2.48	0.83	-0.64	1.74	1.06	-0.77	2.78
PBE0	2.55	-1.42	7.56	0.93	-0.20	2.57	0.83	-0.63	1.84	1.07	-0.77	2.83
MN15	2.63	-1.52	7.88	1.00	-0.24	2.83	0.89	-0.65	2.14	1.15	-0.80	3.13
CAM-B3LYP	2.49	-1.25	7.61	0.99	-0.14	2.63	0.82	-0.62	1.82	1.03	-0.73	2.83
ω B97X-V	2.33	-1.14	7.16	1.01	-0.16	2.70	0.77	-0.57	1.79	1.00	-0.68	2.85
ω B97M-V	2.31	-1.14	7.06	1.00	-0.10	2.56	0.77	-0.58	1.83	1.00	-0.69	2.87

an average RMSE increase of 0.21 kcal/mol. Interestingly, (s)MP3: κ -OOMP2 does not show a similar degradation, leading to perceptibly better performance than tested DFT methods at the sMP3 level.

The A24 set consists of interaction energies of closed shell molecules. MP2:DFT is able to slightly reduce the RMSE relative to MP2:HF (from 0.5 kcal/mol to 0.3-0.4 kcal/mol). A much more significant reduction in error is achieved by sMP2:DFT, which lowers RMSE to 0.1-0.2 kcal/mol. Inclusion of third-order contributions does not significantly improve the already excellent sMP2:DFT predictions, with both MP3:DFT and sMP3:DFT yielding RMSE on the scale of 0.1 kcal/mol as well. However, scaling does improve κ -OOMP2 performance, allowing it to reproduce the benchmark values with lower RMSE than tested DFT methods at the sMP3 level.

Table 9: Root mean square errors (RMSE), mean signed errors (MSE), and maximum absolute errors (MAX) in kcal/mol for MP:DFT on the A24 dataset.

Name	RMSE	MSE	MAX	RMSE	MSE	MAX	RMSE	MSE	MAX	RMSE	MSE	MAX
CCSD	0.25	0.23	0.43									
	MP2			sMP2			MP3			sMP3		
κ -OOMP2	0.20	-0.14	0.60	0.14	0.10	0.33	0.11	0.04	0.37	0.08	0.01	0.24
HF	0.52	0.08	2.41	0.53	0.20	2.43	0.49	0.19	2.20	0.49	0.16	2.26
SPW92	0.50	-0.35	1.87	0.20	0.13	0.47	0.17	0.03	0.48	0.17	-0.02	0.40
PBE	0.43	-0.30	1.60	0.16	0.09	0.43	0.13	-0.01	0.36	0.13	-0.04	0.37
BLYP	0.43	-0.31	1.54	0.15	0.08	0.43	0.11	-0.05	0.25	0.13	-0.08	0.40
B97M-V	0.35	-0.26	1.18	0.13	0.05	0.43	0.12	0.01	0.39	0.12	-0.04	0.30
SCAN	0.38	-0.27	1.34	0.15	0.06	0.46	0.14	0.02	0.43	0.14	-0.02	0.33
revM06-L	0.31	-0.23	1.10	0.14	0.06	0.40	0.13	0.03	0.41	0.11	-0.01	0.30
TPSS	0.38	-0.25	1.40	0.17	0.09	0.43	0.12	0.01	0.35	0.12	-0.02	0.31
B3LYP	0.33	-0.24	1.10	0.14	0.07	0.40	0.10	-0.02	0.29	0.11	-0.05	0.33
PBE0	0.31	-0.23	1.06	0.14	0.06	0.42	0.12	0.02	0.37	0.11	-0.03	0.30
MN15	0.33	-0.26	1.03	0.16	0.08	0.37	0.13	0.02	0.43	0.12	-0.02	0.29
CAM-B3LYP	0.29	-0.22	0.89	0.13	0.07	0.34	0.10	-0.01	0.32	0.10	-0.04	0.27
ω B97X-V	0.26	-0.19	0.80	0.13	0.07	0.31	0.12	0.02	0.38	0.10	-0.02	0.24
ω B97M-V	0.28	-0.22	0.89	0.13	0.07	0.35	0.12	0.01	0.38	0.11	-0.04	0.29

3.2.4 Dipoles

Having examined the performance of MP:DFT on some representative datasets of ground state energetics, we investigated its performance at predicting molecular dipole moments (and thereby densities, indirectly). The dataset from Ref 46 was employed, with the 152 species within being separated into 81 not spin-polarized (NSP) and 71 spin-polarized (SP) cases, depending on whether unrestricted HF broke spin-symmetry or not. For consistency of assessment, the regularized error expression $\frac{\mu - \mu_{\text{ref}}}{\max(\mu_{\text{ref}}, 1 D)} \times 100\%$ (vs CCSD(T) reference value μ_{ref}) from Ref 46 was employed in order to not weigh ionic species with large dipoles or nearly non-polar molecules with small dipoles too heavily.

Table 10 shows that MP2:HF is already quite effective at predicting dipole moments for NSP (i.e. unambiguously closed-shell) species, with a RMS regularized error (RMSRE) of 3.7%, vs 2.8% for CCSD. Similar to many other datasets, MP2:DFT actually degrades performance, with LSDA/GGAs predicting RMSRE > 8%. Rung 3 meta-GGAs have lower

Table 10: Root mean square regularized errors (RMSRE) and mean signed regularized errors (MSRE), in % for MP:DFT on the non spin-polarized (NSP) subset of the dipole dataset.

Name	RMSRE	MSRE	RMSRE	MSRE	RMSRE	MSRE	RMSRE	MSRE
CCSD	2.8	1.6						
	MP2		sMP2		MP3		sMP3	
κ -OOMP2	5.7	-1.1	3.7	0.5	2.6	1.5	1.7	1.0
HF	3.7	1.3	3.5	2.0	3.9	2.5	2.9	2.1
SPW92	8.5	-3.2	4.8	-0.4	2.8	0.9	2.4	0.4
PBE	8.4	-3.1	4.7	-0.4	2.7	0.9	2.3	0.4
BLYP	8.3	-3.1	4.6	-0.3	2.7	0.9	2.3	0.4
B97M-V	6.6	-2.1	4.0	-0.0	2.5	1.2	1.8	0.6
SCAN	7.2	-2.3	4.2	-0.1	2.6	1.1	2.0	0.6
revM06-L	6.4	-1.5	4.0	0.4	2.6	1.4	2.0	0.9
TPSS	7.9	-2.7	4.6	-0.3	2.6	1.0	2.2	0.5
B3LYP	6.6	-1.9	4.0	0.2	2.6	1.2	2.0	0.7
PBE0	6.2	-1.7	3.9	0.2	2.6	1.2	1.9	0.7
MN15	6.0	-1.0	3.8	0.7	2.7	1.5	1.9	1.0
CAM-B3LYP	5.8	-1.2	3.7	0.6	2.7	1.4	2.0	1.0
ω B97X-V	5.5	-0.8	3.7	0.7	2.7	1.5	1.9	1.0
ω B97M-V	5.6	-1.0	3.7	0.6	2.7	1.4	1.9	0.9

RMSRE, and hybrid functionals yield better results still, suggesting that the error is influenced by delocalization error in the reference functional. Nonetheless, neither κ -OOMP2 nor range separated hybrid functionals with low delocalization error (like ω B97X-V) are able to attain MP2:HF level results. sMP2:DFT leads to some improvement, with κ OOMP2 and range separated hybrids attaining (s)MP2:HF level accuracy, but the error still appears to depend on delocalization error in the underlying functional. In contrast, MP3:DFT RMSEs are virtually functional agnostic and represent a significant improvement over MP3:HF, attaining close to (or slightly better than) CCSD level accuracy for all functionals tested. Scaling the third-order term leads to further improvement, with mGGA and hybrid functionals leading to $\sim 2\%$ RMSE, comparable to the best double hybrid density functionals (and much better than predictions from the best hybrid functionals).⁴⁶ κ -OOMP2 orbitals lead to slightly better performance, with an RMSE of 1.7%. It is quite interesting that c_3 scaling parameters trained on W4-11 energies prove to be quite effective for a molecular property like dipole moments (i.e. derivative of the energy vs an applied field).

Table 11: Root mean square regularized errors (RMSRE) and mean signed regularized errors (MSRE) in % for MP:DFT on the spin-polarized (SP) subset of the dipole dataset.

Name	RMSRE MSRE		RMSRE MSRE		RMSRE MSRE		RMSRE MSRE	
CCSD	4.6	2.0						
	MP2		sMP2		MP3		sMP3	
κ -OOMP2	14.5	-2.8	8.9	-0.6	9.4	1.6	8.5	0.8
HF	51.0	14.4	45.6	13.6	29.0	10.0	34.6	11.2
SPW92	14.6	-4.8	7.6	-1.0	6.4	1.3	5.3	0.5
PBE	14.1	-4.3	7.5	-1.1	6.7	1.5	5.6	0.7
BLYP	14.4	-4.4	7.7	-1.0	6.9	1.4	6.0	0.7
B97M-V	13.5	-2.8	7.9	-0.6	7.3	0.5	5.5	-0.1
SCAN	13.1	-3.3	7.0	-0.8	6.2	0.9	4.8	0.3
revM06-L	14.0	-1.9	8.3	0.0	8.0	0.5	5.9	0.1
TPSS	13.3	-3.9	7.1	-0.9	6.1	1.5	5.0	0.8
B3LYP	12.8	-2.5	7.0	-0.2	7.2	1.2	5.7	0.6
PBE0	11.9	-2.2	6.6	-0.2	6.5	1.3	4.9	0.7
MN15	13.4	-2.0	8.1	-0.1	6.7	0.8	5.4	0.3
CAM-B3LYP	11.8	-1.7	6.6	0.2	6.8	1.4	5.3	0.9
ω B97X-V	10.9	-1.3	6.3	0.5	5.9	1.3	4.0	0.8
ω B97M-V	11.5	-1.5	6.6	0.3	6.0	1.2	4.1	0.7

A somewhat different picture is obtained for dipole moments of SP species. Unrestricted MP2 (UMP2) is known to be problematic for prediction of molecular properties, as the one particle density matrix could be non N -representable (i.e. occupation numbers greater than 2 or less than 0) in regions where the orbital rotation hessian is singular (or nearly so).⁹¹ The consequences of this behavior are clearly seen for the SP subset of species, with MP2:HF having an RMSRE of 50%. Use of DFT orbitals significantly reduces spin-contamination, permitting a dramatic reduction of RMSRE to 10-15% for MP2:DFT (which is still significantly larger than the corresponding NSP RMSRE). sMP2:DFT leads to further improvements, leading to 6%-8% RMSRE vs 46% RMSRE with sMP2:HF. Third-order contributions also help reduce error (with the MP3 RMSRE going down relative to MP2) for each orbital choice, and scaling provides some further improvement. However, sMP3:DFT SP RMSREs are still fairly large relative to the corresponding NSP values, and a strong level of functional dependence persists. It is nonetheless encouraging that sMP3: ω B97X-V and sMP3: ω B97M-V marginally outperform CCSD even for the SP dataset. Interestingly, κ -OOMP2 orbitals

yield much worse results for this dataset, with sMP3: κ -OOMP2 having over double the RMSRE of the best sMP3:DFT methods. The most significant instance of MP: κ -OOMP2 failure is prediction of near zero dipole moments for the very challenging NaLi molecule⁴⁶ (vs a CCSD(T) benchmark of 0.59 D). The second most significant case of failure is BH, where (s)MP3: κ OOMP3 predicts a dipole of ~ 2 D vs 1.4 D from CCSD(T). It is also worth noting that there exists a slightly higher energy spin unpolarized (i.e. restricted) κ -OOMP2 solution for both NaLi and BH that leads to much more accurate dipole moments with (s)MP3. It thus appears that sMP3:DFT can be effective for predicting dipole moments for both NSP and SP species (though with much lower error for NSP species), although sMP2:HF is the best $O(N^5)$ scaling approach. It will be interesting to see whether similar behavior holds for other properties like static polarizabilities, where MP2:HF is excellent for NSP species, but more problematic for SP cases.⁹²

3.3 Non-equilibrium configurations

We next examine bond dissociation problems where MP theory is particularly challenged. Orbital degeneracies lead to divergent behavior when restricted orbitals are employed, resulting in catastrophic failure. UMP2 has its own challenges, with a derivative discontinuity in the energy at the Coulson-Fischer (CF) point as well as a discontinuity in first-order (and higher) properties, due to non N -representability of the one particle density matrix.⁹¹ Furthermore, xDH functionals are known to yield unphysical behavior (such as inversion of dipole moments) for highly stretched bonds, due to non-Hellman-Feynman terms coming from the non-perturbative component of the energy (as the orbitals are obtained from another method and are thus not self-consistent).⁹³ The use of non self-consistent orbitals in MP:DFT is thus similarly expected to pose a challenge, making bond dissociations an interesting regime for characterizing the limitations of MP:DFT.

A plot of the MP:DFT dipole moment as a function of bond stretch for the hydrogen fluoride (FH) molecule is shown in Fig 3. The behavior of MP2 without non-Brillouin singles

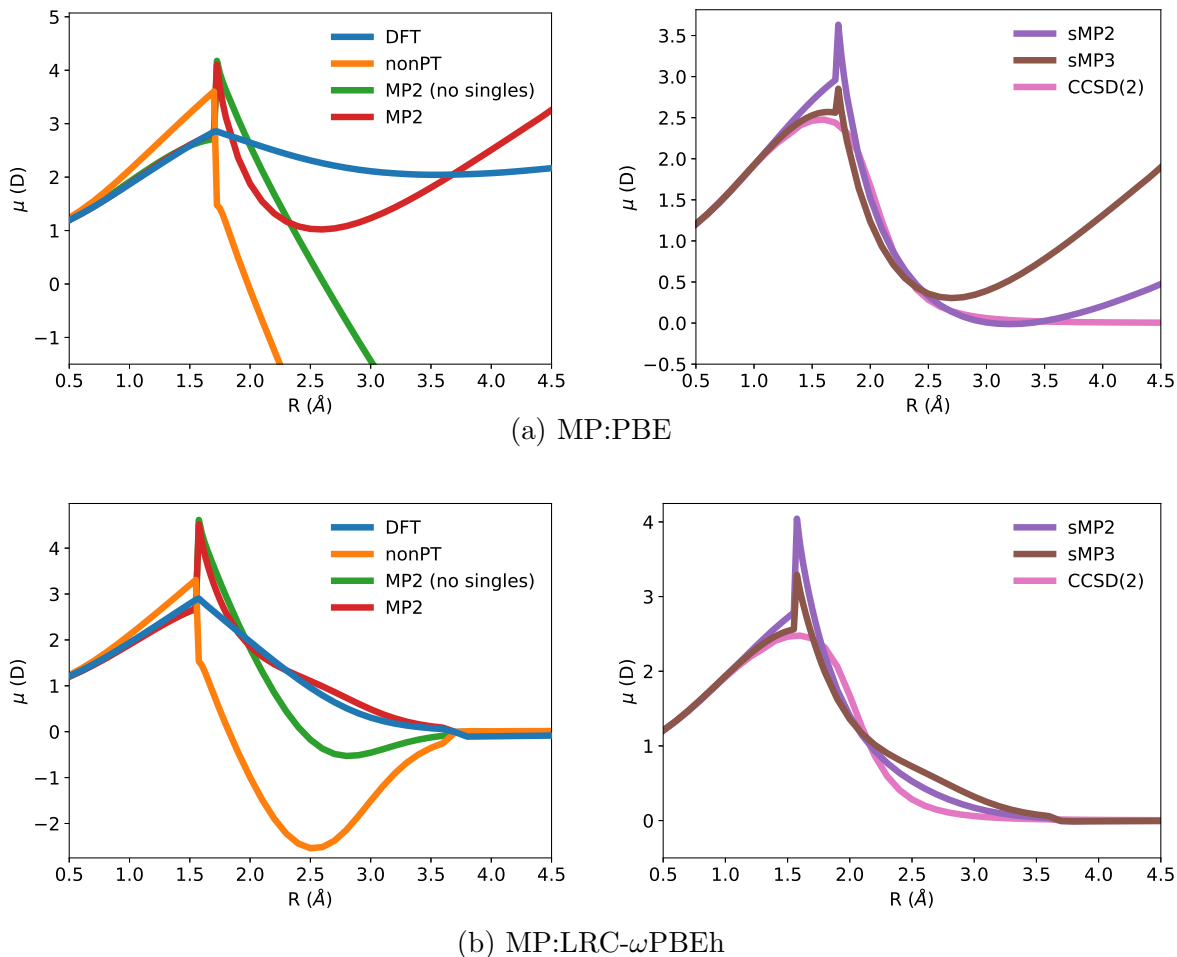


Figure 3: Dipole moments (μ) as a function of internuclear distance (R) for the FH molecule, for various MP:PBE and MP:LRC- ω PBEh approaches. A CCSD(2)⁹ benchmark is also supplied. MP2 (no singles) does not contain non-Brillouin singles, while the non-perturbative (nonPT) approach does not contain any perturbative correction whatsoever (i.e. is obtained from the HF energy computed from DFT densities). MP3:DFT was very similar to sMP3:DFT and was thus not shown separately. A positive value of μ indicates a polarity of H^+F^- .

and the contribution from the non-perturbative (nonPT) terms (i.e. HF:DFT) is also plotted. It can be seen that the MP2 CF point discontinuity is unsurprisingly retained by MP:DFT, though the precise location of the CF point is functional sensitive. It can also be seen that the nonPT models predict unphysically large negative dipole moments at large stretches for all functionals, spuriously indicating a polarity of H^-F^+ . Inclusion of MP2 doubles (i.e. MP2 without non-Brillouin singles) partially ameliorates this, but the qualitatively

problematic behavior persists. This is exactly the behavior seen for xDH functionals, where the non-Hellman-Feynman terms leads to an overcorrection of the delocalization error in the underlying functional.⁹³ Orbitals from functionals with less delocalization error have smaller failures, as can be seen from the relative “success” of the range-separated hybrid LRC- ω PBEh⁹⁴ functional, compared to the local PBE functional.

Interestingly however, the unphysical dipole inversion is eliminated upon inclusion of non-Brillouin singles in MP2, yielding the correct H^+F^- polarity at all distances. While exponentiated single excitations are equivalent to orbital rotation,⁹⁵ it is a little surprising that inclusion of merely the first-order term in the power series of the orbital rotation operator is adequate to address the dipole inversion problem. This does not however mean that MP:DFT is qualitatively successful in the non-equilibrium regime, as the behavior of the models is very functional sensitive. MP:PBE predicts existence of partial charges in the dissociation limit (as can be seen from the asymptotically divergent dipoles in Fig 3a), similar to the behavior predicted by the baseline functional on account of delocalization error.^{46,96,97} Indeed, the dissociation limit partial charges appear to be larger for MP:PBE than PBE itself, based on asymptotic μ divergence rates. The use of local functionals for generating MP:DFT reference orbitals for cases with catastrophic delocalization error is thus clearly problematic, and cannot be recommended.

MP:LRC- ω PBEh does however go to the correct dissociation limit of neutral atoms, similar to the underlying functional. A discontinuity at the CF point is nonetheless retained (in contrast to the derivative discontinuity predicted by the reference DFT functional itself), although reasonable agreement with a CCSD(2)⁹ benchmark is observed at other regimes. Overall however, MP:DFT appears to be ill-suited for non-equilibrium problems like stretched bonds, due to limitations of both standard MP theory and delocalization error from DFT functionals. Even dissociation of nonpolar bonds could prove problematic, as many exchange-correlation functionals yield unphysical behavior for highly stretched nonpolar bonds (relative to unrestricted HF) due to incomplete spin-localization,⁹⁸ making

MP:DFT on such references likely much less optimal than MP:HF.

4 Discussion

The good performance of MP:DFT relative to MP:HF naturally raises questions about the factors that contribute to improved accuracy. A related, but equally intriguing issue is the relatively low impact the choice of the reference functional has on MP3:DFT errors, even in the absence of functional specific scaling factors. Traditional wisdom² would indicate that the main issue with MP:HF is spin-contamination in HF orbitals, leading to unreasonably slow convergence of the MP series. Indeed, we do observe significant reduction of error for datasets like RSE43 or SP dipole moments, where several species are heavily spin-contaminated at the HF level (but not with the functionals studied). However, this cannot be the sole factor as Sec 3.1.3 demonstrated that significant reduction in error is possible even for systems without heavy spin-contamination. Similarly, the A24 results in Table 9 show improved performance vs MP:HF for unambiguously closed-shell species.

Another potential factor behind improved performance could be the higher quality of DFT densities over HF⁴⁶ for molecules at equilibrium. This general idea has precedence in quantum chemistry, with the density-corrected DFT (DC-DFT)^{99,100} approach evaluating DFT energies with HF densities for problems where self-consistent DFT densities are qualitatively problematic (possibly due to delocalization error⁹⁹ or incomplete spin localization⁹⁸). However, improved reference densities are unlikely to be responsible for the success of MP:DFT for many of the datasets studied. The unscaled MP3:PBE and MP3:PBE0 errors are quite similar for the non-barrier height datasets, despite PBE0 predicting significantly more accurate densities than PBE.^{46,101} Similar parallels can be drawn between many other functional pairs, indicating that accurate reference densities are not the most critical factor. This is not to insinuate that reference density quality does not matter at all—the barrier height datasets demonstrate a dependence on delocalization error in the reference functional,

and Fig 3 clearly shows that a catastrophically poor reference is unsalvageable with MP theory. However, even MP3:SPW92 exceeds MP3:HF in accuracy for the two barrier height datasets, showing that factors other than density quality or delocalization error are playing an important role in reducing error.

A third possible contributor is the role of non-Brillouin singles in MP:DFT. MP2 non-Brillouin singles are a major contributor to the worse performance of MP2:DFT relative to MP2:HF (as shown in the Supporting Information), via extra correlation. However, exclusion of singles leads to significantly poorer MP3:DFT performance and considerably greater variation over different functionals. It thus appears that a subtle partial cancellation between MP2 singles and MP3 doubles is responsible for a significant reduction of error at the MP3:DFT level for many functionals, especially LSDA/GGAs. This cancellation also appears to be responsible for the low functional dependence of (s)MP3:DFT. However it is also worth noting that hybrid functionals (especially range separated ones) continue to have lower MP3:DFT errors than MP3:HF even in the absence of MP2 singles, and thus presence of singles cannot be the main factor behind improved performance of MP:DFT for these functionals. Indeed, it does not appear that there is a single obvious factor that is responsible for the greater accuracy of MP:DFT over MP:HF. It is almost easier to conclude that HF orbitals are uniquely poor references for quantitative accuracy with low order MP theory, and almost any DFT approach (or κ -OOMP2) can do significantly better (especially if a close eye is kept on delocalization error or other qualitative failures).

5 Behavior at the Complete Basis Set Limit

We next gauge the practical utility of MP: ω B97M-V by comparison to various density functionals and MP:HF. Comparison to DFT is only meaningful at the CBS limit, due to different basis set convergence rates of MP and DFT. The datasets considered are the nonMR section of W4-11, 24 diverse barrier heights (DBH24,¹⁰² a subset of HTBH38 and NHTBH38)

and TA13. These datasets also contain post CCSD(T) corrections to benchmark values (at least to the CCSDT(Q) level), although such effects could be small in practice (especially for TA13). The c_2 coefficient for sMP2 and c_3 coefficient for sMP3 were reparameterized by fitting to the original benchmark values¹⁰³ of the nonMR W4-11 subset, though the resulting values of 0.8425 and 0.7679 are not too different from the values found from fitting to CCSD(T) for aug-cc-pVTZ (0.8412 and 0.8012 respectively, given in Table 1). The corresponding c_2 and c_3 values for MP:HF are 0.9007 and 0.7060 respectively, again quite close to the values in Table 1 (0.9035 and 0.7157).

Table 12: Root mean square errors (RMSE), mean signed errors (MSE), and maximum absolute errors (MAX) in kcal/mol for MP: ω B97M-V, MP:HF and various DFT approaches. ω B97M(2)²⁰/CBS values were obtained in a similar manner as MP: ω B97M-V/CBS (but without a frozen core correction as the functional was trained without them). Other DFT results and the reference values were obtained from Ref 79.

	nonMR W4-11			DBH24			TA13		
Method	RMSE	MSE	MAX	RMSE	MSE	MAX	RMSE	MSE	MAX
MP2: ω B97M-V	12.2	-4.1	53.5	5.0	-2.5	17.1	2.42	-1.36	7.22
sMP2: ω B97M-V	5.3	-0.8	25.4	2.7	0.0	6.5	0.99	-0.14	2.55
MP3: ω B97M-V	4.2	0.1	17.7	1.8	0.7	6.9	0.79	-0.58	1.74
sMP3: ω B97M-V	2.2	-0.9	8.4	0.8	0.0	1.4	1.10	-0.76	3.01
MP2:HF	12.8	-5.4	58.2	7.2	4.8	19.0	1.97	0.07	5.81
sMP2:HF	11.2	-3.0	50.1	7.4	5.4	18.1	1.79	0.47	4.24
MP3:HF	10.2	-1.0	43.2	6.5	5.1	17.4	1.51	0.44	4.23
sMP3:HF	9.6	-2.3	44.2	6.4	5.0	14.2	1.59	0.33	4.03
BLYP-D3(BJ)	6.7	0.6	31.8	9.6	-8.3	21.3	6.10	-3.99	15.62
PBE-D3(BJ)	10.0	-2.2	42.4	10.4	-8.4	29.7	6.54	-4.66	15.98
SCAN-D3(BJ)	5.5	-0.7	17.5	8.0	-6.9	17.1	4.89	-3.57	11.12
B97M-V	3.8	-1.2	26.7	5.0	-3.7	12.1	4.12	-2.49	9.02
B3LYP-D3(BJ)	3.7	0.3	17.5	5.4	-4.6	9.9	3.85	-2.73	8.99
PBE0-D3(BJ)	4.8	-0.9	20.3	4.7	-3.5	13.3	3.31	-2.45	8.57
ω B97X-V	3.6	0.1	11.9	1.8	-0.1	4.2	2.88	-1.29	8.76
ω B97M-V	2.5	-0.2	11.3	1.5	-0.7	3.9	2.75	-0.98	7.92
ω B97M(2)	1.8	-0.6	7.4	0.7	-0.3	1.4	1.14	-0.53	3.37

Table 12 presents MP:DFT errors for these datasets, along with those of MP:HF and several classic and recent DFT functionals. DFT performs excellently on the nonMR W4-11 subset (as exemplified by the 2.5 kcal/mol RMSE of ω B97M-V), which is relatively un-

surprising⁷⁹ due to the lack of multireference species. On the other hand, MP:DFT is not particularly competitive, with sMP3: ω B97M-V only marginally lowering the RMSE of reference functional despite much larger computational cost ($O(N^6)$ vs $O(N^4)$). MP3: ω B97M-V performs even more poorly, having an RMSE larger than that of the local B97M-V functional. This appears to indicate that there is little practical sense in applying (s)MP3 to problems that are considered to be “easy” for DFT. The ω B97M(2) functional²⁰ performs the best with an RMSE of 1.8 kcal/mol, representing a very reliable approach for thermochemistry calculations with only $O(N^5)$ scaling cost. Nonetheless, (s)MP3: ω B97M-V represents a significant increase in accuracy over (s)MP3:HF.

Presence of delocalization error makes barrier heights considerably more challenging for DFT. Most functionals consequently show significant systematic underestimation of DBH24 barrier heights, bar the range separated (double) hybrid functionals. sMP3: ω B97M-V has significantly lower RMSE than the reference ω B97M-V functional, although MP3: ω B97M-V fares slightly worse. It is also evident that MP:DFT leads to a considerable reduction in RMSE vs MP:HF. However, ω B97M(2) performs equally well as sMP3: ω B97M-V and is the more practical route for accurate barrier height computations for large systems.

The TA13 dataset of radical-closed shell non-covalent interaction energies offers a clear scenario where MP:DFT is superior to existing hybrid DFT approaches, with sMP2: ω B97M-V improving upon the RMSE of ω B97M-V by nearly a factor of 3. Interestingly, MP3: ω B97M-V is the best performer for this dataset, with sMP3 faring slightly worse (similar to behavior for aug-cc-pVTZ, as shown by Table 8). Nonetheless, all MP:DFT methods perform very well, with even unscaled MP2: ω B97M-V being marginally better than the reference functional. Of the DFT methods, only the ω B97M(2) functional is competitive, having essentially the same RMSE as sMP3: ω B97M-V. This is perhaps unsurprising on account of the good performance of sMP2: ω B97M-V, as ω B97M(2) is a more general xDH functional employing the same reference orbitals. The challenges faced by other DFT methods for this dataset are delocalization driven (as multireference character appears small, based on the small magni-

tude of post CCSD(T) corrections for this dataset⁸⁹), permitting MP (and double hybrid) approaches to be more effective. Indeed, routine MP:HF performs reasonably well for this dataset, having RMSEs that are considerably smaller than those predicted by hybrid functionals (though larger than sMP2/(s)MP3: ω B97M-V). It thus appears that (s)MP3:DFT methods are mostly likely to be useful for problems with significant delocalization error, where even modern hybrid density functionals are significantly challenged. However, the great accuracy of MP2 based modern double hybrid functionals likely makes them the more computationally efficient route for investigating such problems than (s)MP3:DFT. On the other hand, these results do seem to suggest that MP3 based double hybrid xDH functionals could potentially be even more accurate.

6 Conclusions and future directions

In this work we have shown that the use of DFT orbitals yields significant improvement to MP2 and MP3 theory, over all functionals and datasets tested. In fact, the choice of the reference functional had surprisingly little overall impact on the error, although hybrid functionals with lower delocalization error appear to have an edge (especially for barrier heights). The exception to this general rule is MP2:DFT, which overcorrelates more than standard MP2 due to presense of non-Brillouin singles, and thus performs worse in most cases (with improvements mostly arising from cases with significant spin-contamination in HF, such as in RSE43). Scaling of the MP2 correlation energy is however adequate for ameliorating the overcorrelation problem, with sMP2:DFT providing significant improvement relative to MP2:DFT over the studied datasets (often reducing RMSE by a factor of 2-3). Nonetheless, modern double hybrid density functionals^{20,21} are likely to offer even better accuracy than sMP2:DFT at the same asymptotic cost (as hinted at by Table 12). It is also quite interesting that the c_2 scaling parameter obtained from fitting to W4-11 thermochemistry proved quite transferable across all datasets, indicating similar levels of MP2 overcorrelation throughout.

MP3:DFT also proved quite robust, with a typical 2-3 fold reduction in RMSE over MP3:HF, even without any scaling. The c_3 scaling parameter obtained from W4-11 was not highly transferable, with slight degradation of performance on going from MP3:DFT to sMP3:DFT in several cases (such as HTBH38). However, the degradation is typically small (0.1-0.2 kcal/mol) while the improvements for datasets like W4-11 and BH76RC are larger, making sMP3:DFT preferable to MP3:DFT for general use. Indeed, MP3:DFT and sMP3:DFT were found to reproduce the CCSD(T) benchmark better than CCSD for several datasets, suggesting that they are quite attractive as $O(N^6)$ scaling wave function methods (especially as multiple $O(N^6)$ iterations are not required, unlike CCSD). (s)MP3:DFT also significantly improves dipole moment predictions relative to MP3:HF, showing success at predicting molecular properties as well. The overall behavior remains mostly functional agnostic (on account of cancellation between MP3 doubles and non-Brillouin MP2 singles), with an edge for hybrid functionals with low delocalization error for challenging problems like barrier heights.

It thus appears that DFT orbitals are better suited than HF orbitals for many practical applications of MP theory. Self-interaction error free κ -OOMP2 orbitals offer a similar improvement in performance, but the lower iterative cost of DFT ($O(N^4)$ for hybrid functionals) would reduce the overall computation time. Furthermore, the near universal availability of DFT and MP features in quantum chemistry packages (relative to OOMP2) would permit wide applicability of any DFT orbital based MP approach. We therefore recommend use of range-separated hybrid DFT or κ -OOMP2 orbitals over HF orbitals for practical use of MP theory. Such reference states would have low delocalization error and thus are likely to be widely applicable. While there have been many studies showing slow or erratic convergence of the MP series,^{2,22-27} it is noteworthy that all of them have used HF orbitals. It may well be interesting to revisit such problems using DFT orbitals to explore whether or not our promising results at 2nd and 3rd order are sustained to higher orders as well.

A purely wave function based MP approach however is unlikely to be competitive with

density functional approaches for ground state computations, even with improved reference orbitals. Indeed, Table 12 indicates that MP:DFT is likely to only significantly improve upon hybrid DFT for problems with significant delocalization error, making DFT preferable for most problems. Furthermore, modern double hybrid functionals like ω B97M(2) are quite competitive with (s)MP3:DFT for even the challenging cases, making them a computationally more efficient route. However, the good performance of sMP3 over sMP2 for many datasets seem to suggest that xDH double hybrid functionals with MP3 correlation could potentially significantly improve upon the best performing modern double hybrids. MP2 geometries are also considered to be quite accurate,¹⁰⁴ indicating that MP:DFT could be a promising route for even more accurate geometries and frequencies at similar cost. This would entail development of analytical nuclear gradients that account for non-Hellman-Feynman terms stemming from lack of self-consistency, which we are currently exploring.

State-specific excited state computations offer another potential application for MP:DFT. Density functional theory based state-specific excited state approaches¹⁰⁵⁻¹⁰⁹ are challenged by the single-determinant nature of Kohn-Sham theory.¹¹⁰ While reasonable recoupling protocols can be devised in certain cases,¹¹¹⁻¹¹³ many states with significantly multiconfigurational nature remain inaccessible with DFT alone. However, excited state-specific MP2 approaches (based on HF orbitals) have also been fairly successful for problems with single configuration state functions.^{114,115} MP:DFT thus appears to be a promising route that could be employed for multiconfigurational problems, via employing non-orthogonal configuration interaction¹¹⁶ based recoupling between single reference states generated via MP^{117,118} from DFT optimized orbitals. Work along these directions is presently in progress.

Acknowledgment

This research was supported by the Director, Office of Science, Office of Basic Energy Sciences, of the U.S. Department of Energy under Contract No. DE-AC02-05CH11231.

References

- (1) Møller, C.; Plesset, M. S. Note on an approximation treatment for many-electron systems. *Phys. Rev.* **1934**, *46*, 618.
- (2) Cremer, D. Møller–Plesset perturbation theory: from small molecule methods to methods for thousands of atoms. *Wiley Interdisciplinary Reviews: Computational Molecular Science* **2011**, *1*, 509–530.
- (3) Raghavachari, K.; Trucks, G. W.; Pople, J. A.; Head-Gordon, M. A fifth-order perturbation comparison of electron correlation theories. *Chem. Phys. Lett.* **1989**, *157*, 479–483.
- (4) Andersson, K.; Malmqvist, P. A.; Roos, B. O.; Sadlej, A. J.; Wolinski, K. Second-order perturbation theory with a CASSCF reference function. *J. Phys. Chem.* **1990**, *94*, 5483–5488.
- (5) Andersson, K.; Malmqvist, P.-Å.; Roos, B. O. Second-order perturbation theory with a complete active space self-consistent field reference function. *J. Chem. Phys.* **1992**, *96*, 1218–1226.
- (6) Harrison, R. J. Approximating full configuration interaction with selected configuration interaction and perturbation theory. *J. Chem. Phys.* **1991**, *94*, 5021–5031.
- (7) Angeli, C.; Cimiraglia, R.; Evangelisti, S.; Leininger, T.; Malrieu, J.-P. Introduction of n-electron valence states for multireference perturbation theory. *J. Chem. Phys.* **2001**, *114*, 10252–10264.
- (8) Angeli, C.; Cimiraglia, R.; Malrieu, J.-P. N-electron valence state perturbation theory: a fast implementation of the strongly contracted variant. *Chem. Phys. Lett.* **2001**, *350*, 297–305.

- (9) Gwaltney, S. R.; Head-Gordon, M. A second-order perturbative correction to the coupled-cluster singles and doubles method: CCSD (2). *J. Chem. Phys.* **2001**, *115*, 2014–2021.
- (10) Guo, S.; Li, Z.; Chan, G. K.-L. A perturbative density matrix renormalization group algorithm for large active spaces. *J. Chem. Theory Comput.* **2018**, *14*, 4063–4071.
- (11) Szabo, A.; Ostlund, N. S. *Modern Quantum Chemistry: Introduction to Advanced Electronic Structure Theory*; Dover Publications, Inc.: Mineola, New York, 1996; pp 286–296.
- (12) Epstein, P. S. The stark effect from the point of view of Schroedinger’s quantum theory. *Phys. Rev.* **1926**, *28*.
- (13) Nesbet, R. K. Configuration interaction in orbital theories. *Proc. R. Soc. A* **1955**, *230*, 312–321.
- (14) Malrieu, J.; Spiegelmann, F. Possible artifacts occurring in the calculation of intermolecular energies from delocalized pictures. *Theoretica chimica acta* **1979**, *52*, 55–66.
- (15) Görling, A.; Levy, M. Exact Kohn-Sham scheme based on perturbation theory. *Phys. Rev. A* **1994**, *50*, 196.
- (16) Grimme, S. Semiempirical hybrid density functional with perturbative second-order correlation. *J. Chem. Phys.* **2006**, *124*, 034108.
- (17) Zhang, Y.; Xu, X.; Goddard, W. A. Doubly hybrid density functional for accurate descriptions of nonbond interactions, thermochemistry, and thermochemical kinetics. *Proc. Natl. Acad. Sci. U.S.A.* **2009**, *106*, 4963–4968.
- (18) Peverati, R.; Head-Gordon, M. Orbital optimized double-hybrid density functionals. *J. Chem. Phys.* **2013**, *139*, 024110.

- (19) Goerigk, L.; Grimme, S. Double-hybrid density functionals. *Wiley Interdisciplinary Reviews: Computational Molecular Science* **2014**, *4*, 576–600.
- (20) Mardirossian, N.; Head-Gordon, M. Survival of the most transferable at the top of Jacob’s ladder: Defining and testing the ω B97M (2) double hybrid density functional. *J. Chem. Phys.* **2018**, *148*, 241736.
- (21) Santra, G.; Sylvetsky, N.; Martin, J. M. Minimally empirical double-hybrid functionals trained against the GMTKN55 database: revDSD-PBEP86-D4, revDOD-PBE-D4, and DOD-SCAN-D4. *J. Phys. Chem. A* **2019**, *123*, 5129–5143.
- (22) Handy, N.; Knowles, P.; Somasundram, K. On the convergence of the Møller-Plesset perturbation series. *Theoretica chimica acta* **1985**, *68*, 87–100.
- (23) Nobes, R. H.; Pople, J. A.; Radom, L.; Handy, N. C.; Knowles, P. J. Slow convergence of the møller-plesset perturbation series: the dissociation energy of hydrogen cyanide and the electron affinity of the cyano radical. *Chem. Phys. Lett.* **1987**, *138*, 481–485.
- (24) Gill, P. M.; Pople, J. A.; Radom, L.; Nobes, R. H. Why does unrestricted Møller–Plesset perturbation theory converge so slowly for spin-contaminated wave functions? *J. Chem. Phys.* **1988**, *89*, 7307–7314.
- (25) Olsen, J.; Christiansen, O.; Koch, H.; Jørgensen, P. Surprising cases of divergent behavior in Møller–Plesset perturbation theory. *J. Chem. Phys.* **1996**, *105*, 5082–5090.
- (26) Leininger, M. L.; Allen, W. D.; Schaefer III, H. F.; Sherrill, C. D. Is Møller–Plesset perturbation theory a convergent ab initio method? *J. Chem. Phys.* **2000**, *112*, 9213–9222.
- (27) Cremer, D.; He, Z. Sixth-Order Møller- Plesset Perturbation Theory On the Convergence of the MP n Series. *J. Phys. Chem.* **1996**, *100*, 6173–6188.

- (28) Pitoňák, M.; Neogrády, P.; Černý, J.; Grimme, S.; Hobza, P. Scaled MP3 non-covalent interaction energies agree closely with accurate CCSD(T) benchmark data. *ChemPhysChem* **2009**, *10*, 282–289.
- (29) Li, C.; Yang, W. On the piecewise convex or concave nature of ground state energy as a function of fractional number of electrons for approximate density functionals. *J. Chem. Phys.* **2017**, *146*, 074107.
- (30) Hait, D.; Head-Gordon, M. Delocalization errors in density functional theory are essentially quadratic in fractional occupation number. *J. Phys. Chem. Lett.* **2018**, *9*, 6280–6288.
- (31) Lochan, R. C.; Head-Gordon, M. Orbital-optimized opposite-spin scaled second-order correlation: An economical method to improve the description of open-shell molecules. *J. Chem. Phys.* **2007**, *126*, 164101.
- (32) Neese, F.; Schwabe, T.; Kossmann, S.; Schirmer, B.; Grimme, S. Assessment of orbital-optimized, spin-component scaled second-order many-body perturbation theory for thermochemistry and kinetics. *J. Chem. Theory Comput.* **2009**, *5*, 3060–3073.
- (33) Kurlancheek, W.; Lochan, R.; Lawler, K.; Head-Gordon, M. Exploring the competition between localization and delocalization of the neutral soliton defect in polyenyl chains with the orbital optimized second order opposite spin method. *J. Chem. Phys.* **2012**, *136*, 054113.
- (34) Grimme, S. Improved second-order Møller–Plesset perturbation theory by separate scaling of parallel-and antiparallel-spin pair correlation energies. *J. Chem. Phys.* **2003**, *118*, 9095–9102.
- (35) Jung, Y.; Lochan, R. C.; Dutoi, A. D.; Head-Gordon, M. Scaled opposite-spin second order Møller–Plesset correlation energy: an economical electronic structure method. *J. Chem. Phys.* **2004**, *121*, 9793–9802.

- (36) Lochan, R. C.; Jung, Y.; Head-Gordon, M. Scaled Opposite Spin Second Order Møller-Plesset Theory with Improved Physical Description of Long-Range Dispersion Interactions. *J. Phys. Chem. A* **2005**, *109*, 7598–7605.
- (37) Grimme, S. Improved third-order Møller–Plesset perturbation theory. *J. Comp. Chem.* **2003**, *24*, 1529–1537.
- (38) Bozkaya, U. Orbital-optimized third-order Møller-Plesset perturbation theory and its spin-component and spin-opposite scaled variants: Application to symmetry breaking problems. *J. Chem. Phys.* **2011**, *135*, 224103.
- (39) Soydas, E.; Bozkaya, U. Assessment of Orbital-Optimized Third-Order Møller–Plesset Perturbation Theory and Its Spin-Component and Spin-Opposite Scaled Variants for Thermochemistry and Kinetics. *J. Chem. Theory Comput.* **2013**, *9*, 1452–1460.
- (40) Soydas, E.; Bozkaya, U. Assessment of orbital-optimized MP2. 5 for thermochemistry and kinetics: dramatic failures of standard perturbation theory approaches for aromatic bond dissociation energies and barrier heights of radical reactions. *J. Chem. Theory Comput.* **2015**, *11*, 1564–1573.
- (41) Lee, J.; Head-Gordon, M. Regularized orbital-optimized second-order Møller–Plesset perturbation theory: A reliable fifth-order-scaling electron correlation model with orbital energy dependent regularizers. *J. Chem. Theory Comput.* **2018**, *14*, 5203–5219.
- (42) Bertels, L. W.; Lee, J.; Head-Gordon, M. Third-Order Møller–Plesset Perturbation Theory Made Useful? Choice of Orbitals and Scaling Greatly Improves Accuracy for Thermochemistry, Kinetics, and Intermolecular Interactions. *J. Phys. Chem. Lett.* **2019**, *10*, 4170–4176.
- (43) Sherrill, C. D.; Lee, M. S.; Head-Gordon, M. On the performance of density functional theory for symmetry-breaking problems. *Chem. Phys. Lett.* **1999**, *302*, 425–430.

- (44) Perdew, J. P.; Parr, R. G.; Levy, M.; Balduz Jr, J. L. Density-functional theory for fractional particle number: derivative discontinuities of the energy. *Phys. Rev. Lett.* **1982**, *49*, 1691.
- (45) Mori-Sánchez, P.; Cohen, A.; Yang, W. Many-electron self-interaction error in approximate density functionals. *J. Chem. Phys.* **2006**, *125*, 201102.
- (46) Hait, D.; Head-Gordon, M. How accurate is density functional theory at predicting dipole moments? An assessment using a new database of 200 benchmark values. *J. Chem. Theory Comput.* **2018**, *14*, 1969–1981.
- (47) Beran, G. J.; Gwaltney, S. R.; Head-Gordon, M. Approaching closed-shell accuracy for radicals using coupled cluster theory with perturbative triple substitutions. *Phys. Chem. Chem. Phys.* **2003**, *5*, 2488–2493.
- (48) Fang, Z.; Lee, Z.; Peterson, K. A.; Dixon, D. A. Use of Improved Orbitals for CCSD (T) Calculations for Predicting Heats of Formation of Group IV and Group VI Metal Oxide Monomers and Dimers and UCl₆. *J. Chem. Theory Comput.* **2016**, *12*, 3583–3592.
- (49) Fang, Z.; Vasiliu, M.; Peterson, K. A.; Dixon, D. A. Prediction of bond dissociation energies/heats of formation for diatomic transition metal compounds: CCSD (T) works. *J. Chem. Theory Comput.* **2017**, *13*, 1057–1066.
- (50) Bertels, L. W.; Lee, J.; Head-Gordon, M. Polishing the Gold Standard: The Role of Orbital Choice in CCSD (T) Vibrational Frequency Prediction. *arXiv preprint arXiv:2007.08435* **2020**,
- (51) Su, N. Q.; Xu, X. The XYG3 type of doubly hybrid density functionals. *Wiley Interdisciplinary Reviews: Computational Molecular Science* **2016**, *6*, 721–747.

- (52) Goerigk, L.; Grimme, S. Efficient and Accurate Double-Hybrid-Meta-GGA Density Functionals Evaluation with the Extended GMTKN30 Database for General Main Group Thermochemistry, Kinetics, and Noncovalent Interactions. *J. Chem. Theory Comput.* **2011**, *7*, 291–309.
- (53) Karton, A.; Daon, S.; Martin, J. M. W4-11: A high-confidence benchmark dataset for computational thermochemistry derived from first-principles W4 data. *Chem. Phys. Lett.* **2011**, *510*, 165–178.
- (54) Dirac, P. A. Quantised singularities in the electromagnetic field. Proc. R. Soc. A. 1931; pp 60–72.
- (55) Perdew, J. P.; Wang, Y. Accurate and simple analytic representation of the electron-gas correlation energy. *Phys. Rev. B* **1992**, *45*, 13244.
- (56) Perdew, J. P.; Burke, K.; Ernzerhof, M. Generalized gradient approximation made simple. *Phys. Rev. Lett.* **1996**, *77*, 3865.
- (57) Becke, A. D. Density-functional exchange-energy approximation with correct asymptotic behavior. *Phys. Rev. A* **1988**, *38*, 3098.
- (58) Lee, C.; Yang, W.; Parr, R. G. Development of the Colle-Salvetti correlation-energy formula into a functional of the electron density. *Phys. Rev. B* **1988**, *37*, 785.
- (59) Mardirossian, N.; Head-Gordon, M. Mapping the genome of meta-generalized gradient approximation density functionals: The search for B97M-V. *J. Chem. Phys.* **2015**, *142*, 074111.
- (60) Sun, J.; Ruzsinszky, A.; Perdew, J. P. Strongly Constrained and Appropriately Normed Semilocal Density Functional. *Phys. Rev. Lett.* **2015**, *115*, 036402.
- (61) Wang, Y.; Jin, X.; Haoyu, S. Y.; Truhlar, D. G.; He, X. Revised M06-L functional for

- improved accuracy on chemical reaction barrier heights, noncovalent interactions, and solid-state physics. *Proc. Natl. Acad. Sci. U.S.A.* **2017**, *114*, 8487–8492.
- (62) Tao, J.; Perdew, J. P.; Staroverov, V. N.; Scuseria, G. E. Climbing the density functional ladder: Nonempirical meta-generalized gradient approximation designed for molecules and solids. *Phys. Rev. Lett.* **2003**, *91*, 146401.
- (63) Becke, A. D. Density-functional thermochemistry. III. The role of exact exchange. *J. Chem. Phys.* **1993**, *98*, 5648–5652.
- (64) Adamo, C.; Barone, V. Toward reliable density functional methods without adjustable parameters: The PBE0 model. *J. Chem. Phys.* **1999**, *110*, 6158–6170.
- (65) Haoyu, S. Y.; He, X.; Li, S. L.; Truhlar, D. G. MN15: A Kohn–Sham global-hybrid exchange–correlation density functional with broad accuracy for multi-reference and single-reference systems and noncovalent interactions. *Chem. Sci.* **2016**, *7*, 5032–5051.
- (66) Yanai, T.; Tew, D. P.; Handy, N. C. A new hybrid exchange–correlation functional using the Coulomb-attenuating method (CAM-B3LYP). *Chem. Phys. Lett.* **2004**, *393*, 51–57.
- (67) Mardirossian, N.; Head-Gordon, M. ω B97X-V: A 10-parameter, range-separated hybrid, generalized gradient approximation density functional with nonlocal correlation, designed by a survival-of-the-fittest strategy. *Phys. Chem. Chem. Phys.* **2014**, *16*, 9904–9924.
- (68) Mardirossian, N.; Head-Gordon, M. ω B97M-V: A combinatorially optimized, range-separated hybrid, meta-GGA density functional with VV10 nonlocal correlation. *J. Chem. Phys.* **2016**, *144*, 214110.
- (69) Dunning, T. H. Gaussian basis sets for use in correlated molecular calculations. I. The atoms boron through neon and hydrogen. *J. Chem. Phys.* **1989**, *90*, 1007–1023.

- (70) Kendall, R. A.; Dunning, T. H.; Harrison, R. J. Electron affinities of the first-row atoms revisited. Systematic basis sets and wave functions. *J. Chem. Phys.* **1992**, *96*, 6796–6806.
- (71) Woon, D. E.; Dunning, T. H. Gaussian basis sets for use in correlated molecular calculations. III. The atoms aluminum through argon. *J. Chem. Phys.* **1993**, *98*, 1358–1371.
- (72) Woon, D. E.; Dunning Jr, T. H. Gaussian basis sets for use in correlated molecular calculations. V. Core-valence basis sets for boron through neon. *J. Chem. Phys.* **1995**, *103*, 4572–4585.
- (73) Helgaker, T.; Klopper, W.; Koch, H.; Noga, J. Basis-set convergence of correlated calculations on water. *The Journal of chemical physics* **1997**, *106*, 9639–9646.
- (74) Halkier, A.; Helgaker, T.; Jørgensen, P.; Klopper, W.; Koch, H. et al. Basis-set convergence in correlated calculations on Ne, N₂, and H₂O. *Chemical Physics Letters* **1998**, *286*, 243–252.
- (75) Pritchard, B. P.; Altarawy, D.; Didier, B.; Gibson, T. D.; Windus, T. L. New basis set exchange: An open, up-to-date resource for the molecular sciences community. *Journal of chemical information and modeling* **2019**, *59*, 4814–4820.
- (76) Shao, Y.; Gan, Z.; Epifanovsky, E.; Gilbert, A. T.; Wormit, M. et al. Advances in molecular quantum chemistry contained in the Q-Chem 4 program package. *Mol. Phys.* **2015**, *113*, 184–215.
- (77) Feyereisen, M.; Fitzgerald, G.; Komornicki, A. Use of approximate integrals in ab initio theory. An application in MP2 energy calculations. *Chem. Phys. Lett.* **1993**, *208*, 359–363.

- (78) Bernholdt, D. E.; Harrison, R. J. Large-scale correlated electronic structure calculations: the RI-MP2 method on parallel computers. *Chem. Phys. Lett.* **1996**, *250*, 477–484.
- (79) Mardirossian, N.; Head-Gordon, M. Thirty years of density functional theory in computational chemistry: an overview and extensive assessment of 200 density functionals. *Mol. Phys.* **2017**, *115*, 2315–2372.
- (80) Najibi, A.; Goerigk, L. The nonlocal kernel in van der Waals density functionals as an additive correction: An extensive analysis with special emphasis on the B97M-V and ω B97M-V approaches. *J. Chem. Theory Comput.* **2018**, *14*, 5725–5738.
- (81) Goerigk, L.; Grimme, S. A general database for main group thermochemistry, kinetics, and noncovalent interactions - Assessment of common and reparameterized (meta-)GGA density functionals. *J. Chem. Theory Comput.* **2010**, *6*, 107–126.
- (82) Zhao, Y.; Lynch, B. J.; Truhlar, D. G. Multi-coefficient extrapolated density functional theory for thermochemistry and thermochemical kinetics. *Phys. Chem. Chem. Phys.* **2005**, *7*, 43–52.
- (83) Zhao, Y.; González-García, N.; Truhlar, D. G. Erratum: Benchmark database of barrier heights for heavy atom transfer, nucleophilic substitution, association, and unimolecular reactions and its use to test theoretical methods (J. Phys. Chem. A (2005) 109A (2015-2016)). **2006**, *110*, 4942.
- (84) Andreas Gansäuer, Radicals in Synthesis I. In *Radicals in Synthesis I*; Springer-Verlag, 2006.
- (85) Goerigk, L.; Hansen, A.; Bauer, C.; Ehrlich, S.; Najibi, A. et al. A look at the density functional theory zoo with the advanced GMTKN55 database for general main group thermochemistry, kinetics and noncovalent interactions. *Phys. Chem. Chem. Phys.* **2017**, *19*, 32184–32215.

- (86) Boese, A. D.; Martin, J. M. Development of density functionals for thermochemical kinetics. *J. Chem. Phys.* **2004**, *121*, 3405–3416.
- (87) Lynch, B. J.; Fast, P. L.; Harris, M.; Truhlar, D. G. Adiabatic connection for kinetics. *J. Phys. Chem. A* **2000**, *104*, 4811–4815.
- (88) Kang, J. K.; Musgrave, C. B. Prediction of transition state barriers and enthalpies of reaction by a new hybrid density-functional approximation. *J. Chem. Phys.* **2001**, *115*, 11040–11051.
- (89) Tentscher, P. R.; Arey, J. S. Binding in radical-solvent binary complexes: Benchmark energies and performance of approximate methods. *J. Chem. Theory Comput.* **2013**, *9*, 1568–1579.
- (90) Řezáč, J.; Hobza, P. Describing noncovalent interactions beyond the common approximations: How accurate is the "gold standard," CCSD(T) at the complete basis set limit? *J. Chem. Theory Comput.* **2013**, *9*, 2151–2155.
- (91) Kurlancheek, W.; Head-Gordon, M. Violations of N -representability from spin-unrestricted orbitals in Møller–Plesset perturbation theory and related double-hybrid density functional theory. *Mol. Phys.* **2009**, *107*, 1223–1232.
- (92) Hait, D.; Head-Gordon, M. How accurate are static polarizability predictions from density functional theory? An assessment over 132 species at equilibrium geometry. *Phys. Chem. Chem. Phys.* **2018**, *20*, 19800–19810.
- (93) Hait, D.; Head-Gordon, M. Communication: xDH double hybrid functionals can be qualitatively incorrect for non-equilibrium geometries: Dipole moment inversion and barriers to radical-radical association using XYG3 and XYGJ-OS. *J. Chem. Phys.* **2018**, *148*, 171102.

- (94) Rohrdanz, M. A.; Martins, K. M.; Herbert, J. M. A long-range-corrected density functional that performs well for both ground-state properties and time-dependent density functional theory excitation energies, including charge-transfer excited states. *J. Chem. Phys.* **2009**, *130*, 054112.
- (95) Thouless, D. Stability conditions and nuclear rotations in the Hartree-Fock theory. *Nuclear Physics* **1960**, *21*, 225–232.
- (96) Ruzsinszky, A.; Perdew, J. P.; Csonka, G. I.; Vydrov, O. A.; Scuseria, G. E. Spurious fractional charge on dissociated atoms: Pervasive and resilient self-interaction error of common density functionals. *J. Chem. Phys.* **2006**, *125*, 194112.
- (97) Dutoi, A. D.; Head-Gordon, M. Self-interaction error of local density functionals for alkali-halide dissociation. *Chem. Phys. Lett.* **2006**, *422*, 230–233.
- (98) Hait, D.; Rettig, A.; Head-Gordon, M. Well-behaved versus ill-behaved density functionals for single bond dissociation: Separating success from disaster functional by functional for stretched H₂. *J. Chem. Phys.* **2019**, *150*, 094115.
- (99) Kim, M.-C.; Sim, E.; Burke, K. Understanding and reducing errors in density functional calculations. *Phys. Rev. Lett.* **2013**, *111*, 073003.
- (100) Kim, M.-C.; Sim, E.; Burke, K. Ions in solution: Density corrected density functional theory (DC-DFT). *J. Chem. Phys.* **2014**, *140*, 18A528.
- (101) Brorsen, K. R.; Yang, Y.; Pak, M. V.; Hammes-Schiffer, S. Is the Accuracy of Density Functional Theory for Atomization Energies and Densities in Bonding Regions Correlated? *J. Phys. Chem. Lett.* **2017**, *8*, 2076–2081.
- (102) Karton, A.; Tarnopolsky, A.; Lamère, J.-F.; Schatz, G. C.; Martin, J. M. Highly accurate first-principles benchmark data sets for the parametrization and validation of density functional and other approximate methods. Derivation of a robust, generally

- applicable, double-hybrid functional for thermochemistry and thermochemical kinetics. *The Journal of Physical Chemistry A* **2008**, *112*, 12868–12886.
- (103) Karton, A.; Daon, S.; Martin, J. M. W4-11: A high-confidence benchmark dataset for computational thermochemistry derived from first-principles W4 data. *Chem. Phys. Lett.* **2011**, *510*, 165–178.
- (104) Curtiss, L. A.; Raghavachari, K.; Redfern, P. C.; Rassolov, V.; Pople, J. A. Gaussian-3 (G3) theory for molecules containing first and second-row atoms. *J. Chem. Phys.* **1998**, *109*, 7764–7776.
- (105) Gilbert, A. T.; Besley, N. A.; Gill, P. M. Self-consistent field calculations of excited states using the maximum overlap method (MOM). *J. Phys. Chem A* **2008**, *112*, 13164–13171.
- (106) Kowalczyk, T.; Yost, S. R.; Voorhis, T. V. Assessment of the Δ SCF density functional theory approach for electronic excitations in organic dyes. *J. Chem. Phys.* **2011**, *134*, 054128.
- (107) Kowalczyk, T.; Tsuchimochi, T.; Chen, P.-T.; Top, L.; Van Voorhis, T. Excitation energies and Stokes shifts from a restricted open-shell Kohn-Sham approach. *J. Chem. Phys.* **2013**, *138*, 164101.
- (108) Barca, G. M.; Gilbert, A. T.; Gill, P. M. Simple Models for Difficult Electronic Excitations. *J. Chem. Theory Comput.* **2018**, *14*, 1501–1509.
- (109) Hait, D.; Head-Gordon, M. Excited state orbital optimization via minimizing the square of the gradient: General approach and application to singly and doubly excited states via density functional theory. *J. Chem. Theory Comput.* **2020**, *16*, 1699–1710.
- (110) Kohn, W.; Sham, L. J. Self-consistent equations including exchange and correlation effects. *Phys. Rev.* **1965**, *140*, A1133.

- (111) Ziegler, T.; Rauk, A.; Baerends, E. J. On the calculation of multiplet energies by the Hartree-Fock-Slater method. *Theoretica chimica acta* **1977**, *43*, 261–271.
- (112) Frank, I.; Hutter, J.; Marx, D.; Parrinello, M. Molecular dynamics in low-spin excited states. *J. Chem. Phys.* **1998**, *108*, 4060–4069.
- (113) Hait, D.; Haugen, E. A.; Yang, Z.; Oosterbaan, K. J.; Leone, S. R. et al. Accurate prediction of core-level spectra of radicals at density functional theory cost via square gradient minimization and recoupling of mixed configurations. *arXiv preprint arXiv:2006.10181* **2020**,
- (114) Carter-Fenk, K.; Herbert, J. M. State-Targeted Energy Projection: A Simple and Robust Approach to Orbital Relaxation of Non-Aufbau Self-Consistent Field Solutions. *J. Chem. Theory Comput.* **2020**,
- (115) Ye, H.-Z.; Van-Voorhis, T. Self-consistent Møller-Plesset Perturbation Theory For Excited States. *arXiv preprint arXiv:2008.10777* **2020**,
- (116) Thom, A. J.; Head-Gordon, M. Hartree-Fock solutions as a quasidiabatic basis for nonorthogonal configuration interaction. *J. Chem. Phys.* **2009**, *131*, 124113.
- (117) Yost, S. R.; Head-Gordon, M. Size consistent formulations of the perturb-then-diagonalize Møller-Plesset perturbation theory correction to non-orthogonal configuration interaction. *J. Chem. Phys.* **2016**, *145*, 054105.
- (118) Yost, S. R.; Head-Gordon, M. Efficient implementation of NOCI-MP2 using the resolution of the identity approximation with application to charged dimers and long C-C bonds in ethane derivatives. *J. Chem. Theory Comput.* **2018**, *14*, 4791–4805.